UCLouvain

École polytechnique de Louvain

Towards artificial sensory feedback for lower-limb amputees

How does a vibrotactile stimulation of the patellar tendon influence the gait pattern of able-bodied subjects?

Author: **Virginie Otlet**
Supervisor: **Renaud Ronsse**
Readers: **Aleksandar Jankovski**, **Philippe Lefèvre**, **André Mouraux**
Academic year 2018–2019
Master [120] in Biomedical Engineering

Abstract

Context The number of amputations continues to increase due to the ageing population and its associated increase in diabetes. Approximately 85% of these amputations are those of the lower-limb [1]. The lack of sensory feedback provided by existing lower-limb prostheses, in addition to the loss of motor functions, leads to abnormal gait kinematics which cause a lot of additional medical conditions and high risk of falling. A lot of studies have been performed in the past twenty years to increase knowledge in this field.

Objective The goal of this thesis is twofold: to investigate the effects of an artificial sensory feedback on the gait pattern of able-bodied subjects, and to study the effects of a perturbation introduced into this feedback on the gait pattern of these subjects. This thesis is part of the long term objective to develop a lower-limb prosthesis delivering artificial sensory feedback to the user.

Experiments A vibrotactile stimulation is applied at the patellar tendon of the knee with three different conditions: at the maximum knee flexion, 5% of the gait cycle before this event and 5% of the gait cycle after this event. The control condition corresponds to the case where there is no stimulation applied.

Results The statistical analysis shows that there is no effect of the different stimulation conditions on temporal parameters, like the stride durations and the phase leads between legs. In contrast, they have an effect on spatial parameters. Indeed, the amplitudes of the shank angular velocity and vertical acceleration signals are higher for the condition where there is no stimulation applied than the one where the stimulation is applied at the maximum knee flexion. Surprisingly, there is no significant effect of both conditions where the stimulation is applied with an offset.

Remerciements

Je tiens à remercier toutes les personnes qui ont contribué de près ou de loin à la réalisation de ce mémoire.

Ainsi, je voudrais remercier dans un premier temps mon promoteur, Monsieur Renaud Ronsse, pour sa disponibilité, son encadrement et ses conseils tout au long de l'année.

Je tiens également à témoigner ma reconnaissance aux personnes suivantes :

Monsieur Aleksandar Jankovski pour ses conseils quant aux expériences et à l'interprétation des résultats.

Monsieur Julien Lebleu pour son aide concernant l'implémentation du code C#, l'utilisation des IMUs, ainsi que pour ses nombreux conseils.

Monsieur Thierry Daras pour le montage des unités vibrotactiles et pour sa disponibilité.

Madame Sophie Heins qui m'a aidé dans la correction du code Matlab sur les oscillateurs adaptatifs.

Madame Giulia Liberati, Monsieur Cedric Lenoir et Monsieur Alexis Lheureux pour leurs explications sur les unités vibrotactiles et les IMUs.

Madame Christine Detrembleur qui m'a permis d'accéder au laboratoire de la marche.

Le centre Revitalis, et en particulier Monsieur Martin Dayez, pour m'avoir autorisée à utiliser leur tapis de course lorsque le laboratoire n'était pas disponible.

Finalement, j'aimerais remercier ma famille et mes amis, pour avoir accepté de participer à mes expériences, pour avoir relu et corrigé mon mémoire, et surtout pour leur soutien durant toutes mes études.

Contents

List of abbreviations

AOs	Adaptive oscillators
CNS	Central nervous system
CoP	Center of pressure
CPG	Central pattern generator
EMSSA	Electrotactile moving sensation for sensory augmentation
FA	Fast adapting
FSR	Force-sensing resistors
GG	Greenhouse-Geisser correction
HF	Huynd-Feldt correction
HyVE	Hybrid vibro-electrotactile stimulation
IMUs	Inertial Measurement Units
LLA	Lower-limb amputees
SA	Slow adapting
VT	Vibrotactile

List of figures

List of tables

Introduction

With the ageing population and its associated increase in diabetes, the number of amputees is expected to double by 2050, and the major part of these amputations are those of the lower-limb [1, 2]. Nowadays, lower-limb prosthesis unfortunately do not provide any sensory feedback to the user. Abnormal gait kinematics observed in lower-limb amputees due to the loss of motor functions is worsened by this lack of sensory feedback. These abnormal gait patterns cause a lot of additional medical conditions, like osteoarthritis, osteoporosis and back pain. Moreover, there is a high risk of falling and a high rejection rate by patients.

Searchers realized this need of adding an artificial sensory feedback to lower-limb prostheses. A lot of studies have been conducted in the past twenty years to increase knowledge in this field. This thesis is the continuation of the work of Isabelle de Thysebaert [3].
To contribute to the research in this topic, this thesis has two objectives: to observe if an artificial sensory feedback influences the gait pattern of able-bodied subjects, and to study if a perturbation introduced in this feedback also influences their gait pattern. In order to do this, a vibrotactile stimulation of the patellar tendon of the knee is used, and the perturbation takes the form of an offset in the delivering time of the stimulation. Although the experiments were conducted on able-bodied subjects, if we can show that our stimulation can modify their gait pattern, these results could also be used later with lower-limb amputees.

This work is composed of the following structure. In Chapter 1, the context is explained to show why adding a sensory feedback to lower-limb prostheses is of interest. Moreover, some theoretical backgrounds are given to better understand what will be studied. The somatosensory system will be described, as well as the different phases of a normal gait cycle. Finally, the objectives of this work will be defined.

In Chapter 2, the literature about artificial sensory feedback for lower-limb amputees will be reviewed. This chapter focusses on vibrotactile and electrotactile stimulations. It also contains parts about the effects of these stimulations on proprioception and about rehabilitation of lower-limb amputees by adaptation to a perturbation.

In Chapter 3, all the materials and methods are described. This chapter explains the stimulation characteristics chosen based on some articles of the literature review of Chapter 2. It also describes the experimental protocol and the use of adaptive oscillators in order to activate the stimulation. It finishes by explaining the steps for data processing and statistical analysis.

In Chapter 4, the results of the statistical analysis described in the previous chapter will be exposed. Finally, these results are discussed in Chapter 5.

Chapter 1

Context and theoretical background

This chapter will firstly describe the context in which this work takes place. Thereafter, some useful definitions for the understanding of what will follow are given. This second section is divided into three parts: firstly, the heart of this work, the somatosensory feedback, will be explained; then, the gait cycle will be defined; finally, the role of the somatosensory feedback in locomotion will be described to better understand the issues associated to its loss in lower-limb amputees.

1. Motivations

In 2005, the estimated number of amputees, both of the upper- and lower-limb, was about 1.6 million people in the United States. This number is expected to reach 3.6 million by 2050. This augmentation is caused by the ageing population and its associated increase in diabetes, which is one of the main causes of amputation. Indeed, the causes are vascular disease (54%) like diabetes and peripheral arterial disease, trauma (45%) and cancer ($< 2\%$) [2][1].

Approximately 85% of limb amputations are those of the lower-limb [1], that can be performed at different levels (Figure 1). From wooden legs to robotic prostheses, passing by carbon fibre running prostheses for athletes, there have been a lot of improvements in prosthetic lower-limbs. However, one challenge left in this domain is the ability to provide artificial somatosensory feedback (see Section 2.1 for an extended definition). This issue has already been explored for upper-limb prostheses and may have potential solutions [5, 6, 7]. However, while it has also been studied for lower-limb prostheses, the development of a device seems to be less advanced for this ap-

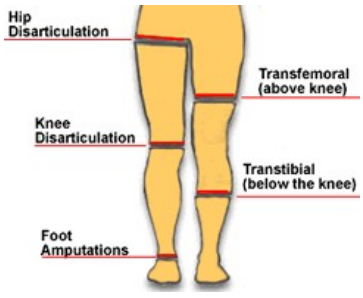

Figure 1: *Levels of lower-limb amputations [4].*

[1] Numbers of 2005.

plication.

Adding artificial sensory feedback to prostheses is a really important aspect because humans rely on somatosensory feedback to control their balance and movement. Therefore, to compensate this lack of information about their prosthetic limb, lower-limb amputees (LLA) rely instead on the sensations coming from the interaction between their stump and their socket, vision and hearing. However, these modalities are not sufficient and amputees develop compensatory strategies leading to abnormal gait kinematics [8, 9], also caused by the loss of motor functions. They use much more their intact limb, inducing asymmetry between their legs, either while walking or standing. They put much more stress on their intact limb, that can cause osteoarthritis of the knee and/or hip joints. As their residual limb bones are not subject to sufficient loading, they can suffer from osteoporosis of this leg. This asymmetry can also lead to back pain [10]. In addition, LLA have a poor balance and postural control, resulting in an increased risk of falling [8]. Moreover, the use of a prosthesis increases the cognitive effort, which causes a high rejection rate by the patient [9]. It also increases the energy consumption, as the gait kinematic is inefficient [1]. In order to improve well-being and quality of life of LLA, artificial sensory feedback should be provided by prostheses, in a similar way as a sound limb does.

2. Theoretical background

2.1. Somatosensory system

The somatosensory system is composed of three subsystems [11]:

- **Touch**: transmits information about fine touch, vibration and pressure thanks to cutaneous mechanoreceptors;
- **Proprioception**: gives information about the position of body parts in space thanks to receptors localized into muscles, tendons and joints;
- **Nociception**: receives information about painful stimuli and changes in temperature.

For the purpose of this work, it only focusses on the two first subsystems. Information is transmitted from receptors to the central nervous system (CNS) by afferent fibres (Table 1). These fibres differentiate from each other by three parameters: their diameter, their conduction velocity and the presence of a myelin sheath. There are three main categories: fibres A (largest and fastest axons), B and C (smallest and slowest). The notation changes for muscle afferent axons, which are classified in four groups: fibres I (the fastest), II, III and IV (the slowest) [11].

Table 1: *Characteristics of somatosensory afferent fibres, adapted from [11].*

Sensory function	Mechanoreceptor type	Afferent axon type	Axon diameter	Conduction velocity
Proprioception	Muscle spindle	Ia, II	13-20 μm	80-120 m/s
Touch	Merkel, Meissner, Pacinian, Ruffini cells	Aβ	6-12 μm	35-75 m/s

Mechanoreceptors specialized for proprioception are shown in Table 2. Muscle spindles are composed of intrafusal muscle fibers on which two types of sensory afferents are connected to transmit sensory information. On the one hand, type Ia provides information about the velocity and direction of the movement. On the other hand, type II transmits information about the static position of limbs. In addition, Golgi tendon organs are located inside tendons to provide information about tension in the muscle. Finally, some mechanoreceptors are also located inside joints to transmit information about the position of the limb [11].

Table 2: *Characteristics of proprioceptive mechanoreceptors [11].*

	Muscle spindle		Golgi tendon organs	Joint receptors
	Ia	**II**	**Ib**	
Location	Parallel to extrafusal muscle fibres, coiled around the central part of intrafusal fibres	Parallel to extrafusal muscle fibres, connected to the end of intrafusal muscle fibers	Inside tendons, in series with extrafusal muscle fibres	Inside joints, resemble to Pacinian and Ruffini corpuscles
	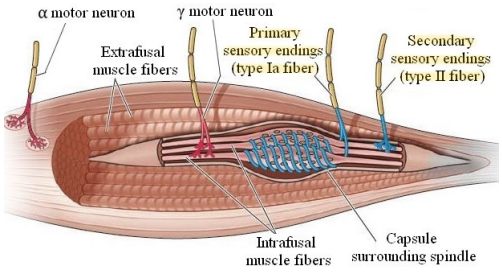		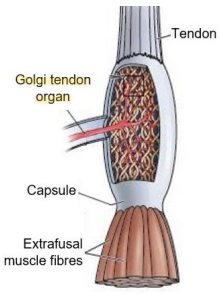	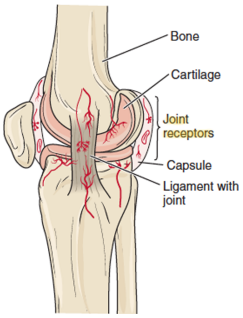 [12]
Function	Detection of changes in muscle length	Detection of the state of the muscle	Detection of changes in muscle tension	Estimating the position of the limb

Cutaneous mechanoreceptors specialized for touch are shown in Table 3. They are characterized by two important aspects [11]:

- **Their speed of adaptation**: fast adapting (FA) receptors fire quickly at the stimulus onset and keep quiet when the stimulus continues. Slow adapting (SA) receptors discharge continuously during all the stimulus. This influences the type of tactile information it will convey: FA will provide informations about changes in stimulus, *i.e.* its movement, while SA about its spatial characteristics, *i.e.* size and shape;
- **The size of their receptive fields**, which is the skin surface over which a stimulation will change the firing of the neuron associated to this surface. It is important in defining the accuracy of the sensation of the tactile stimulus. If receptive fields are small, two close point stimuli can more easily be discriminated, on the contrary of large receptive fields.

Table 3: *Characteristics of cutaneous mechanoreceptors, adapted from [13].*

	Meissner (FA-I)	**Merkel (SA-I)**	**Pacini (FA-II)**	**Ruffini (SA-II)**
Location under the skin	Superficial 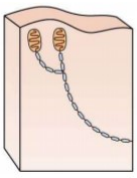	Superficial 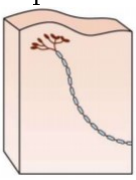	Deep 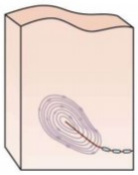	Deep 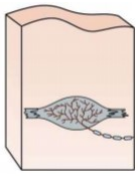
Speed of adaptation	Fast adaptation 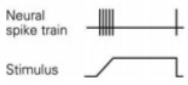	Slow adaptation 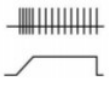	Fast adaptation 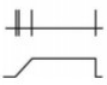	Slow adaptation 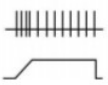
Size of the receptive fields	Small, sharp borders 	Small, sharp borders 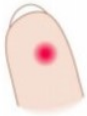	Large, obscure borders 	Large, obscure borders 
Function	Detection of motions on the skin	Distinction of form and texture	Detection of vibrations	Detection of finger movements

2.2. Normal gait cycle

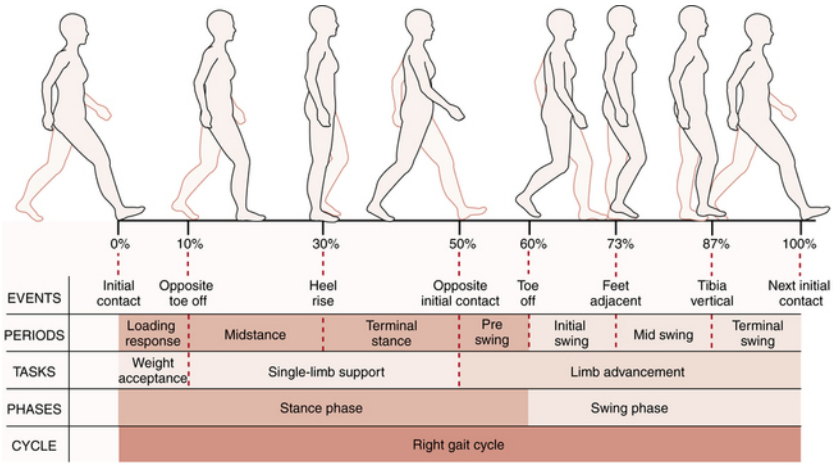

Figure 2: *Gait cycle of the right leg decomposed into events, periods and phases [14].*

The gait cycle is composed of two phases (Figure 2): the **stance phase**, where the foot is in contact with the ground, and the **swing phase**, where it is off the ground [14]. In the following description, the ipsilateral leg is the one of which the gait cycle is studied (here the right leg), and the contralateral leg is the opposite one.

There is firstly the stance phase, decomposed into four periods [14, 1]:

1. **Loading response**: starts when the heel strikes the ground and ends when all the ipsilateral foot is on the ground and the contralateral one starts to takes off the ground. In this phase, the lower extremity accepts the body weight;
2. **Midstance**: ends when the ipsilateral heel leaves the ground;
3. **Terminal stance**: ends when the contralateral heel strikes the ground. During the midstance and this phase, all the body weight is supported by the ipsilateral leg;
4. **Pre-swing**: ends when the ipsilateral foot leaves the ground.

Then follows the swing phase, composed of three periods [14, 1]:

5. **Initial swing**: ends when both feet are next to each other;
6. **Mid swing**: ends when the ipsilateral tibia is perpendicular to the ground;
7. **Terminal swing**: ends when the ipsilateral heel strikes the ground again and the gait cycle therefore restarts. The role of the pre-swing period and of the swing phase is to move the ipsilateral leg forward. During these periods, the body weight is supported by the contralateral leg.

2.3. Role of the somatosensory feedback in locomotion

Human locomotion relies on two important aspects: basic locomotor patterns and feedback mechanisms. The first one is generated by central pattern generators (CPGs) in the spinal cord. Feedback signals allow to adapt these locomotor patterns to the environment. This mechanism is only an assumption for the moment and is not completely validated yet.

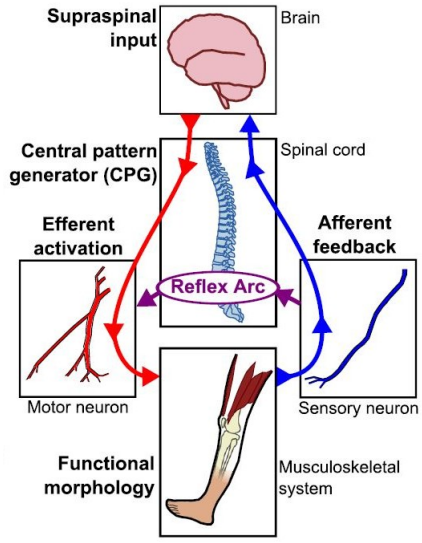

Figure 3: *Sensory-motor closed loop for human locomotion. The sensory afferent signals are in blue and motor efferent signals are in red, adapted from [15].*

There are two main loops used for locomotion (Figure 3): the reflex arc and the supraspinal loop. The first one uses somatosensory feedback to modulate basic locomotor patterns to enhance efficiency of gait under normal conditions and when facing unexpected perturbations. In this last case, provided somatosensory signals from the leg do not match the prediction made by the CNS, leading to an error signal. Therefore, reflex bursts are generated to rapidly correct the movement [16].
In the supraspinal loop, some regions of the brain (premotor and motor cortices, cerebellum and brain stem) combine sensory, visual, auditory and vestibular feedback signals to control balance, orientation and precise foot placement [15].

Once motor commands are sent to muscles, the movement is performed. Then proprioceptive and sensory signals are sent to the brain to give a feedback about the result of the executed movement. Therefore, this forms a sensory-motor closed loop [15]. In LLA, this loop is broken, which leads to the problems mentioned in Section 1.

3. Objectives of this work

This thesis is part of the long term objective to develop a lower-limb prosthesis delivering artificial sensory feedback to the user, in order to replace the lost information coming from the amputated limb. To contribute to research in this field, the questions it will try to answer are:

How does an artificial sensory feedback influence the gait pattern of able-bodied subjects?

and

How does a perturbation introduced into this artificial sensory feedback influence the gait pattern of able-bodied subjects?

The perturbation introduced into the artificial feedback consists in an offset of the delivering time of the stimulation (see Section 2 of Chapter 3 on page 35 for more details).

In this work, tests were performed on able-bodied subjects because we wanted to be sure that they give some useful results before making the experiments with LLA, which is more complicated. Indeed, the gait signal is more regular in able-bodied subjects than in LLA, so the algorithm to detect a particular gait event is less difficult. Moreover, there is less risk of falling during the experiments with able-bodied subjects than with LLA. Therefore, it was preferable to firstly validate our hypotheses on able-bodied subjects and then to confirm these results on LLA.

If this work shows some results on the gait pattern of able-bodied subjects, it can be adapted to LLA by adapting the gait event detection algorithm to their particular gait signal. Depending on our results, it could be used in LLA for rehabilitation, to restore gait symmetry between both legs. Finally, in the future, the fact that an artificial sensory feedback influences the gait pattern of able-bodied subjects could be used in the development of a prosthesis providing this type of feedback to LLA.

Chapter 2

Literature review

This chapter summarizes the articles on artificial sensory feedback for LLA. It allows to observe how the feedback was applied in previous studies, its location and its parameters. This will guide the choices for the experiments of this work. It also allows to see what results can be expected from these stimulations. This chapter also summarizes the effects of stimulations on proprioception and of a perturbation on gait rehabilitation in LLA.

Firstly, all the techniques used to provide an artificial sensory feedback are quickly explained. Then, the literature review focusses on the electrotactile and vibrotactile stimulations only, since this was previously identified as the most relevant modalities for this kind of experiment [3]. For studies about the other techniques for delivering artificial sensory feedback, the reader is referred to the literature review of [3]. Secondly, the effects of vibrotactile and electrical stimulations on proprioceptive feedback are explained. Finally, the motor learning by adaptation to a perturbation is covered, firstly by giving some theoretical concepts and then by discussing its effects on gait rehabilitation in LLA.

1. Artificial feedback for lower-limb amputees

1.1. Overview

A way to improve gait balance and kinematic for LLA is to add an artificial sensory feedback to their prosthesis. There are two ways to use sensory feedback: either for rehabilitation, where the patient has to pay attention to a biomechanical variable during rehabilitation training, or for a permanent use in everyday life, where the patient has to integrate the feedback into its body control scheme [9].

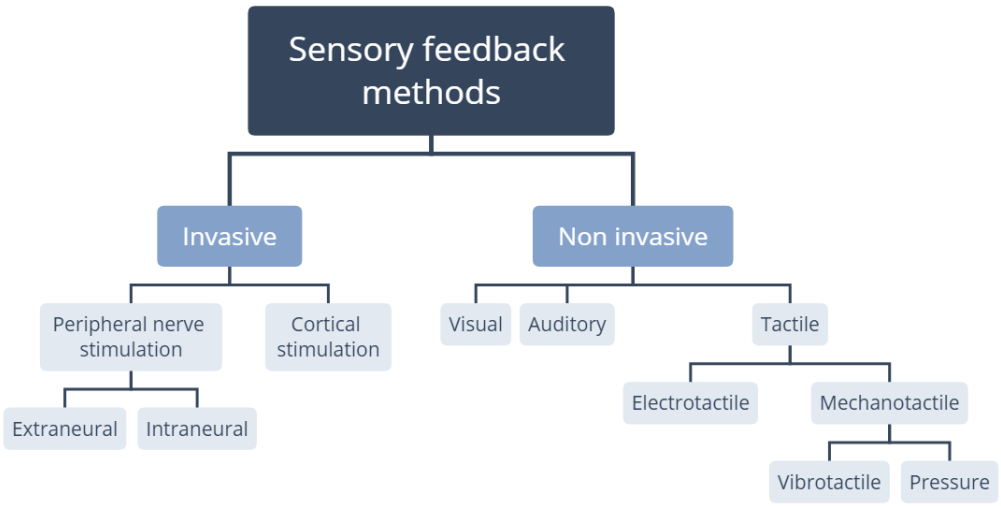

Figure 4: *Diagram summarizing the different techniques providing a sensory feedback, based on [17].*

There exists different methods to provide sensory feedback to amputees (Figure 4), divided into two categories: invasive and non-invasive. Invasive techniques consist in implanted electrodes delivering an electrical stimuli. These electrodes can be implanted at different locations:

- Peripheral nerve stimulation: an electrode is implanted either next to a nerve of the peripheral nervous system (extraneural) or into this kind of nerve (intraneural) [18];
- Cortical stimulation: electrodes are directly implanted in the somatosensory cortex [19].

Non-invasive techniques can be decomposed into several modes:

- Visual: cues containing information about gait characteristics are either projected on a screen or on the ground, or presented through virtual reality or on a smartphone [15];
- Auditory: speakers or headphones give information to the patient by varying characteristics of the presented cues (stereo balance, pitch, timbre, volume) [15];
- Tactile: information is transmitted via variation in frequency, strength, duration, pattern and/or location of cutaneous stimuli. It can be induced in two ways:
  - Electrotactile: an electrical current flows through the skin to evoke a tactile sensation [20];
  - Mechanotactile: there is a displacement of the skin [21], either thanks to a vibration or thanks to an applied pressure.

A comparison of these non-invasive stimulation methods is given in Table 4.

Table 4: *Comparison between non-invasive techniques to provide an artificial sensory feedback.*

	Pros	**Cons**
Visual	– Preferred by patients [15] – Widely tested and good results obtained [15]	– Increase in cognitive load [15] – Non portable systems [15]
Auditory	– Portable systems [15] – Widely tested and good results obtained [15]	Increase in cognitive load which can be dangerous in everyday life [15]
Tactile	No overloading of sensory channels [22]	Subject to adaptation [23]

1.2. Electrotactile stimulation

In a first study about tactile stimuli in 1994 [24], Sabolich and Ortega analysed the effects of a non-invasive sensory feedback device, *Sense-Of-Feel*, on gait quality and efficiency of lower-limb amputees. This device was composed of sensors placed under the heel and under the toe of the prosthetic limb, connected to electrodes placed on the posterior and anterior sides of the stump respectively [25]. The authors collected external measures (weight distribution, standing balance, symmetry of stance phase duration) for their analysis. Their results showed an improvement in symmetry in weight distribution, step length and stance time. The company Sabolich Prosthetic & Research Center, for which this study was conducted, never put that system on the market but is currently developing a Sensory Feedback System to be integrated in their prosthesis [26].

However, despite the usefulness of electrical sensory feedback for lower-limb amputees demonstrated by this study, it was not used for prostheses during a decade because of adaptation induced by prolonged electrical stimulation. Adaptation is characterized by a decreasing response of the action potentials of the sensory system to a constant stimulus [27]. A study of Kaczmarek in 2000 [27] showed that adaptation to continuous electrotactile stimulation happens after 15 min.
This is why Buma and colleagues [23] investigated the influence of different electrotactile stimulation settings on adaptation in 2007. They first analysed the effects of different current

amplitudes of continuous stimulation and then the effects of intermittent stimulation. The stimulation was applied through adhesive cutaneous electrodes, delivering charge-balanced biphasic stimulation pulses, applied just above the knee on the inner thigh of healthy subjects. Their results confirmed those of Kaczmarek. Moreover, they found that adaptation after 15 min was reduced when using intermittent stimulation with a high stimulation current.

Webb [29] presented in 2009 a real-time biofeedback training system first for re-education therapy and maybe later for an everyday use. This device contained an optical motion capture system to measure lower-limb kinematic data through markers placed on the subject. It sent electrotactile stimuli through an array of electrodes placed inside the prosthesis. The stimuli moved around the thigh while the patient was walking.
In a follow-up paper [28], Webb and colleagues described in more details the activation pattern of the electrodes. Their device was developed to minimize circumduction or abduction gait patterns frequently observed in LLA. The stimulus was activated if the gait of the patient moved outside predefined limits. A deviation vector was defined between the normal position of the thigh and its actual position (Figure 5). The angle of this vector determined which electrode was activated and its magnitude determined the stimulus intensity.

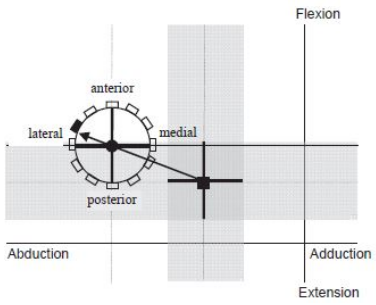

Figure 5: *Electrode selection for the study of Webb [28]. The cross with the square represents the mean and standard deviation of normal sagittal and coronal hip angles at an instant in the gait cycle. The cross with the circle represents hip angles of the patient undergoing training.*

In a study of 2010, Pfeifer and colleagues [30] exploited a particular phenomenon: when a pair of stimuli is applied at different locations and same intensity, a single illusory stimulus is felt between them. If their intensities change, the illusory stimulus moves towards the stronger stimulus. This is called the *phantom sensation phenomenon* or *tactile phi phenomenon* and it allows to send information perceived like continuously moving with only two stimulation locations. Pfeifer and colleagues investigated discrimination between electrotactile phantom sensations to determine if they can be used to encode the location of the center of pressure (CoP) of the foot. The sensation was applied thanks to two pairs of electrotactile stimulators separated by a small distance and delivering biphasic square pulses. The multilayer hydrogel electrodes were placed on the lower back of healthy subjects. The areas between electrodes defined five regions corresponding to regions on the foot. In the first experiment, subjects were asked to identify where on the foot the stimulation they felt was coming from. In the second experiment, they were asked to determine the start and end points of moving patterns corresponding to locomotor activities. Their results showed that subjects were able to identify quite accurately foot regions and dynamic patterns.

In another study of 2012 [31], Webb and colleagues wanted to determine a comfortable range of electrotactile stimulations on the thigh. For this, they used eight electrodes equidistantly distributed around the thigh of healthy subjects, delivering a stimulus of 40, 60 or 80 Hz with increasing intensity. Subjects were asked to say when they found the sensation uncomfortable. The range between mean sensation and discomfort levels decreased with frequency and was lower when patients are laying supine (30.5 to 24.4 mA) than when they are walking (37.8 to 32 mA). This indicated that with higher frequencies, the difference between discomfort and sensation was smaller but however there is a separation. This is important in prostheses because the stimulus can never be felt as uncomfortable.

In their study of 2016 [22], Pagel and colleagues investigated Electrotactile Moving Sensation for Sensory Augmentation (EMSSA), which exploited the same phenomenon as Pfeifer and his colleagues in their study of 2010, *i.e.* the tactile phi phenomenon. They suggested that it allowed to use continuous spatial feedback, which may reduce sensory adaptation and increase transmission efficiency. The CoP under the prosthetic foot was calculated from data provided by a force/moment sensor. The knee and hip joint angles were given by a goniometer-gyroscope sensor system. The stimulation was delivered by two pairs of electrodes placed on the lower back of unilateral transfemoral amputee subjects. They tested a CoP feedback and a knee angle feedback. By exploiting the tactile phi phenomenon, subjects could feel the movement of their CoP moving from heel to toe or the progressive extension of their leg. Their results showed that the use of EMSSA induced a less effective and less efficient postural control and increased cognitive load. However, the experiments were conducted without training of the subjects, which can explain this negative outcome. Therefore, this feedback system may have benefits after a training phase and in the long run.

1.3. Vibrotactile stimulation

The first device using a vibrotactile stimulation for artificial sensory feedback in LLA was the one presented by Zambarbieri and colleagues in 2001 [32]. It consisted in an insole containing two force-sensing resistors (FSR) placed at the heel and at the toe of amputees and of two vibrators placed on the thigh for below-knee amputees and on the trunk for above-knee amputees. The stimulus location gave information to the user about the foot contact on the ground. The results of their first experiments on below-knee amputee subjects showed that they easily accepted the device and it seemed that it helped them during the rehabilitation process by providing them information about their foot pressure.

The study of Wentink and colleagues in 2011 [33] aimed at testing three aspects: the perception of stimuli of different frequencies and locations, the estimation of the number of stimuli and their locations (discrimination between simultaneous or sequential stimuli) and

the habituation to the vibrotactile stimulation. The stimuli were applied on the thigh of healthy subjects through eight pager motors. The first experiment showed that higher frequencies (60-80 Hz) were better perceived at all locations on the thigh and that the medial and posterior sides of the thigh better discriminate between different frequencies. In the second experiment, sequential stimulation was better interpreted by subjects in comparison to simultaneous stimulation. Finally, the time before habituation was longer for vibrotactile stimulation (half-life = 300 s) than for electrotactile stimulation (half-life = 185 s). Therefore, the authors concluded that sequential stimulation was suitable to provide feedback to lower-limb amputees.

In their study of 2012 [34], Rusaw and his colleagues analysed the effects of a vibrotactile stimulation on static and dynamic balance in unilateral transtibial amputee subjects. Vibrating tactors located proximally on the thigh stimulated it proportionally to signal received from pressure sensors placed under the prosthetic foot. Unfortunately, the results showed that this additional feedback gave no particular benefit to prosthetic users. However, this study demonstrated that there was a change in LLA's strategy from feedback to feed-forward mechanisms, *i.e.* that they used information from previous gait cycles to select corrective actions for subsequent gait cycles. Therefore, this type of setup can be used for anticipatory feed-forward mechanisms of postural control.

To better understand the design variables for artificial feedback systems, Sharma and colleagues [8] investigated in 2014 different ways of providing sensory information to LLA by assessing the reaction time and the accuracy of the elicited response. This article is the first one to highlight the importance of a short reaction time for artificial sensory feedback systems to produce fluid movements. The sensory reaction time is defined as "the duration between application of the stimulus and initiation of the response" [8]. The design variables studied were location and frequency of the stimulus, the number of stimuli and the means for subjects to provide their response. The stimuli were applied to the thigh of 12 non-disabled subjects and three transfemoral amputee subjects through vibrotactile motors. The conclusions of the article were as follows. Firstly, the anterior location on the thigh gave quicker reaction times than for the lateral, medial and posterior locations. This is in part due to the faster conduction speed of the anterior femoral cutaneous nerve compared to the lateral and posterior one. Secondly, frequencies that were better detected for skin vibration were around 250 Hz, which corresponds to the activation of Ruffini cylinder and Pacinian corpuscles. Larger frequencies (> 200 Hz) also allowed a better discrimination between frequencies. Finally, when participants had to do a more complex task, as with multiple stimuli or multiple responses, the reaction times increased. Therefore, the authors concluded that such techniques for providing sensory feedback were not suitable for gait and mobility applications. Indeed, given the complexity of gait, it would introduce delays. However, feed-forward systems, *i.e* that use information from previous gait cycles to predict appropriate corrective

actions in a subsequent gait cycle, could be a solution to these delays.

In a subsequent study in 2016 [35], Sharma and colleagues further investigated reaction time and accuracy of the subject response to stimuli. There were applied by the same device than in their previous study and on the same participants, but this time in the presence of a cognitive load and a liner between the skin and the vibrotactile motor. Indeed, LLA sustain a higher cognitive load due to the loss of proprioceptive and sensory information about their lost limb, which can impact their ability to use the artificial sensory feedback. Moreover, the vibrotactile stimulation will be applied through the surface of the prosthesis on the residuum of the patient, it is therefore important to analyse the influence of these liners on the mechanical transmission of the signal. The results showed that both conditions increased the reaction times, and that increasing the cognitive load increased them more than adding a liner.

In their article, Crea and colleagues [9] presented a new device that worked as follows. A discrete vibrotactile stimulation was applied at three locations around the thigh of able-bodied subjects through vibrotactile units. These stimuli were applied synchronously with three gait-phase transitions (heel strike, flat foot and toe off), each location on the thigh corresponding to one transition. These ones were detected through a sensorized prosthetic foot sole. The advantage of using a discrete stimulation is that the rhythm that it creates can be associated with a physiological gait pattern, without additional cognitive load.
The experiments of the authors aimed at determining if the subject detected vibrations while walking and how the detection thresholds changed if the stimulus was not synchronous with a specific gait-phase transition, *i.e.* delayed by 200 or 500 ms corresponding to a possible delay in the wireless communication. Moreover, they investigated if subjects associated the right vibrotactile unit to the right gait-phase transition. Their conclusions were firstly that the device gave information about the timing of gate-phase transitions even in the presence of delays, and secondly that subjects quickly learned to associate vibrotactile units to a specific gait-phase transition.

A subsequent study in 2017 [36] aimed at validating the help provided by the device developed by Crea and colleagues for patients to improve their gait symmetry. For this purpose, the vibrotactile stimulation was applied this time on the lower abdomen of transfemoral amputee subjects and visual feedback was provided during a training session. The visual feedback indicated the stance duration of the two legs and a score comparing the gait symmetry of the subject to a reference value. The conclusions of the article were that associating visual and vibrotactile feedbacks for training substantially improved the gait symmetry of subjects, even when the visual one was not given anymore. They also showed that vibrotactile feedback did not increase the cognitive load as it has been integrated in the walking scheme.

The 2016 study of Wan and colleagues [37] developed a device that provided different vibrotactile patterns for different floor conditions. The device was composed of force sensors placed under the prosthetic foot and vibrators attached to the surface of the hand of five lower-limb amputee subjects and eight healthy subjects. Depending on the location of the object under the prosthetic foot, one of the four vibrators was activated and the subject had to answer if there was an object and where it was. The authors showed that when biofeedback was applied, there was no difference between amputee and non-amputee subjects in detecting the presence and location of the object.

Plauché and colleagues [38] studied in 2016 the feasibility of a haptic system aiming at improving dynamic gait in transfemoral amputees. Their device contained an insole with FSR communicating with linear resonant actuator motors placed equidistantly around the thigh of able-bodied subjects to provide a vibrotactile stimulation. They tested two feedback strategies: (1) a continuous stimulation mapped the displacement of the CoP and (2) a discrete stimulation was applied in the direction of error in CoP. The authors showed that their device improved gait stability and that results were better with the discrete stimulation.

In their article of 2016 [39], Chen, Fen and Wang made the link between myoelectric control of prosthesis and artificial feedback in order to improve prosthetic joint control. For the vibrotactile stimulus, they used pager motors placed on the anterior and posterior sides of the thigh of eight able-bodied subjects and two transtibial amputee subjects. They made several experiments. The two first ones analysed the sensitivity of the thigh to position or amplitude changes in the stimulation. The last one concerned the control of a virtual ankle through EMG signals of dorsiflexor and plantar flexor muscles. The subjects were asked to reach target ankle angles thanks to the feedback provided, either visual or vibrotactile. For the visual feedback, the movement of the ankle was shown on a screen, while for vibrotactile feedback the change of vibration positions indicated to the subject if he had to decrease or increase muscle contraction. Their results showed that control of a virtual ankle with vibrotactile feedback was as good as with visual feedback. However, this last one is not appropriate for everyday life as patients need their visual channel for other activities.

The study of Lauretti and colleagues [40] in 2017 had two objectives: (1) to investigate if vibrotactile feedback can improve balance control in lower-limb amputees and (2) to evaluate the potentiality of the vibrotactile perception as a mean to restore the knee-joint proprioception of LLA.
The experiment to assess the first objective used FSR placed under the sole of 16 healthy subjects and one LLA subject and vibrotactile actuators placed either on their forearm or on their lower back. In this experiment, subjects had to stand on a moving platform and to control their posture thanks to different types of sensory feedback: augmented visuo-proprioceptive feedback, vibrotactile feedback on the forearm, vibrotactile feedback on the

lower back or no feedback. Augmented visuo-proprioceptive feedback consisted in providing to the subject a real-time visual feedback about his center of mass and CoP, in addition to his visual proprioceptive information. This experiment showed that the vibrotactile feedback had better performance than no feedback and that it was comparable to the augmented visuo-proprioceptive feedback.
For the second objective, two types of vibrotactile stimulations were used, both using the tactile phi phenomenon described in Section 1.2. In the continuous vibrotactile feedback, the motion of the subject's knee-joint was linked to the moving stimulus provided by two vibrotactile actuators. The same principle was applied in the discrete vibrotactile feedback, but it used three vibrotactile actuators. It allowed the patient to feel a more intense sensation than with the first feedback. For the experiment, subjects had to reach angular positions with their right knee-joint by exploiting the provided vibrotactile feedback. The conclusions of the authors were that performances obtained with these two types of feedback were higher than with no feedback. However, no significant difference was found between discrete and continuous vibrotactile feedbacks, as well as between the positioning of the vibrotactile actuators either on the forearm or on the lower back.

1.4. Bimodal stimulation

Although only developed for the upper-limb so far, a hybrid vibro-electrotactile stimulation (HyVE) is interesting. Indeed, D'Alonzo and colleagues [21, 41] thought that it can be simultaneously delivered in parallel and at the same skin location but be perceived independently by subjects. This can be explained by the fact that vibrotactile and electrotactile stimulations activate different skin receptors. The advantage of HyVE interface is that it is more compact than two separated feedback interfaces, since they stimulate the same skin area. Moreover, it can be used either to increase the resolution of one feedback variable or to simultaneously give two feedback variables. The device developed by D'Alonzo and colleagues in their studies of 2014 was composed of vibration motors placed on the top of a concentric electrode and the stimulation was applied to the glabrous skin of the forearm of healthy subjects. Their studies showed that HyVE allowed for a better transmission of discrete information than separated vibrotactile or electrotactile stimulations [21] and that it can be used to provide multi-channel sensory information with better performances than these two stimulation modalities separately [41].

1.5. Summary

In all these studies, subjects had to associate the location of the stimulus to a particular gait event. It seems that this characteristic is specific to non-invasive feedback techniques, since it is common to electrotactile and vibrotactile stimulations.

Table 5: *Summary of articles about artificial sensory feedback.*

Source	*Stimulation device*	*Stimulated area*	*Conclusions*
Electrotactile stimulation			
Sabolich and Ortega, 1994 [24]	Cutaneous electrodes	Thigh	Increased gait quality and efficiency
Buma et al. 2007 [23]	Bipolar cutaneous electrodes	Thigh	Adaptation to continuous stimulation arrives after 15 min while it is reduced with intermittent stimulation
Webb et al. 2009-2010 [29, 28]	Array of cutaneous electrodes	Thigh	Development of a device to minimize circumduction or abduction gait patterns
Pfeifer et al. 2010 [30]	Two pairs of multilayer hydrogel electrodes	Lower back	Identification of regions and dynamic patterns with tactile phi phenomenon
Webb et al. 2012 [31]	Cutaneous electrodes	Thigh	Comfortable range of stimulation: laying supine = 24.4 to 30.5 mA; walking = 32 to 37.8 mA
Pagel et al. 2016 [22]	Two pairs of cutaneous electrodes	Lower back	Less effective and less efficient postural control and increased cognitive load with EMSSA
Vibrotactile stimulation			
Zambarbieri et al. 2001 [32]	Vibrators	Thigh or trunk	Easily accepted by patients and helpful during rehabilitation
Wentink et al. 2011 [33]	Pager motors	Thigh	Investigatation of discrimination between stimulus frequencies and locations
Rusaw et al. 2012 [34]	Vibrating tactors	Thigh	No particular benefits on static and dynamic balance
Sharma et al. 2014, 2016 [8, 35]	Vibrotactile motors	Thigh	Reaction times were shorter for anterior location on thigh and longer for more complex task and with a liner between skin and stimulus

Table 5: *Summary of articles about artificial sensory feedback (continuation).*

Source	*Stimulation device*	*Stimulated area*	*Conclusions*
Vibrotactile stimulation (continuation)			
Crea et al. 2015 [9]	Vibrotactile units	Thigh	Quick learning of association between stimulus and specific gait-phase transition
Crea et al. 2017 [36]	Vibrotactile units	Lower abdomen	Association of visual and vibrotactile feedbacks improves gait symmetry without increasing cognitive load
Wan et al. 2016 [37]	Vibrators	Hand	Good detection of presence and location of an object under the foot
Plauché et al. 2016 [38]	Linear resonant actuator motors	Thigh	Increased gait stability and better results when discrete stimulation was used
Chen et al. 2016 [39]	Pager motors	Thigh	Good control of a virtual ankle with vibrotactile feedback
Lauretti et al. 2017 [40]	Vibrotactile actuators	Forearm or lower back	Improved balance control in LLA and restoration of their knee-joint proprioception
Hybrid stimulation			
D'Alonzo et al. 2014 [41, 21]	Vibration motors placed on the top of a concentric electrode	Forearm	Better performances than with the two separate feedback interfaces

For the electroctatile stimulation, the stimulus transmitted some information about the gait characteristics, *i.e.* location of the CoP, foot pressure or knee angle, by the activation of electrodes placed at a specific location on the patient. He had therefore to associate this stimulus to the value of the gait parameter to which it corresponds. Most of these results showed that patients can effectively do this, and some also showed that it can improve gait quality in LLA. Concerning the characteristics of the feedback, discrete stimulation is better than continuous one because of the adaptation to electrotactile stimulus. Moreover, the stimulations were applied either on the thigh or on the lower back. Finally, the tactile phi phenomenon (see Section 1.2) is interesting to decrease the number of needed electrodes, but its effects have still to be studied because of the negative results of the study of Pagel and colleagues [22].

For the vibrotactile stimulation, a lot of the overviewed studies used sensors placed under the prosthetic foot at the heel and toe to send stimulation on the thigh or lower back at locations corresponding to those under the foot, to give information about the foot contact on the ground. Another interesting aspect is the study of reaction times, which showed that they increased with the number of stimuli, which is associated with an increase in cognitive load for the user. A few studies showed that the use of a discrete stimulation instead of a continuous one allows to decrease this cognitive load since the subject integrate the stimulus in his walking scheme quickly. It is also interesting to notice that the tactile phi phenomenon explained for electrotactile stimulation can also be used for vibrotactile stimulation. The general conclusion is that vibrotactile feedback gave good results to improve gait quality and to restore proprioception of the knee and of the ankle joints. It also gave similar results than visual feedback but is more appropriate for everyday life.

A comparison between all these studies is summarized in Table 5 on page 21-22.

2. Effects of a stimulation on proprioceptive feedback

2.1. Vibrotactile stimulation

Some studies about vibrotactile stimulations not applied to LLA give however insightful results for this thesis. Indeed, the fact that a stimulation can influence the proprioceptive feedback in able-bodied subjects can be used to provide an artificial sensory feedback to LLA.

In a study of Verschueren and coworkers in 2002 [42], the effects of tendon vibration on joint kinematics and on intralimb and interlimb coordination were analysed. They placed cylindrical vibrators at several locations on the right leg of subjects:

- On the proximal tendon just under the anterior superior iliac spines for the rectus femoris vibration (thigh);

- On the patellar tendon for the quadriceps vibration at the knee (thigh);
- On the muscle belly of the biceps femoris (thigh) for the vibration of this muscle at the hip and on the distal tendon for the vibration of this muscle at the knee;
- On the tendon of the tibialis anterior for the vibration of the tibialis anterior/extensor digitorum vibration (ankle);
- On the Achilles tendon for the triceps surae vibration (calf).

The subjects had to walk with one vibration's location activated per trial. Joint kinematics were recorded thanks to reflective surface markers placed at several locations. The results showed that the vibration of the quadriceps femoris at the knee decreased knee flexion at the mid swing phase, that vibration of the tibialis anterior decreased plantar flexion at the toe off phase, and that vibration at the triceps surea decreased dorsiflexion during the swing phase. These movements were shortened because of the lengthening illusion of the muscle induced by the vibration, that caused the subject to conclude his movement earlier. Finally, the vibrations on the stimulated leg did not induce any effect on joint displacement of the non-stimulated leg.

In the experiment of Albert and colleagues in 2006 [43], primary muscle spindles, *i.e.* Ia afferent fibres, were stimulated with real patterns of muscle tendon vibration to induce an illusory movement. The vibrotactile stimuli were applied through electromagnetic vibrators on the tendons of the left ankle joint and followed patterns mimicking the natural ones of Ia afferent fibres. Subjects were asked to name the movement that they perceived and then to copy it with their hand. The results showed that an illusory movement can be induced by stimulating primary muscle spindle afferents and that it can be recognized and named. Moreover, vibration stimuli with high mean frequency induced an illusory movement of larger size. Finally, vibration at the natural frequency of Ia afferent fibres (30 Hz), which is lower than frequencies previously defined to perceive more clearly illusory movements (80-100 Hz), also induced it.

In a subsequent study released in 2009, Roll, Albert and colleagues [44] developed a model that mimicked proprioceptive inputs based on recordings of Ia afferent fibres. They made the same experiments as in the previous study with vibration patterns recorded by microneurography, but also with vibration patterns given by their model to compare the results. They showed that the illusory trajectories were identical in both cases, therefore validating their model. Moreover, it can be applied to other joints than the ankle by specifying the preferred sensory direction of joint muscles. For example, applying the vibration patterns on the wrist induced the same illusory trajectories than on the ankle.

Mildren and Bent [45] proved in 2016 that tactile and proprioceptive signals are linked. Their experiments consisted in investigating if vibrotactile stimulations at different locations

on the foot could influence proprioception of the ankle joint. Vibration targets FA receptors, *i.e.* Meissner and Pacinian corpuscules, with frequencies of 45 and 255 Hz respectively. Participants had to determine when their right ankle, passively rotated, was at the same angle than the left ankle, passively put at a target angle. Vibrotactile stimuli were applied through custom made pads shaped to the foot and at one of the three locations. Their results showed that stimulation of foot skin effectively influenced proprioception of the ankle joint, particularly with heel vibration and plantar flexion of the ankle, since the error between correct and real angles increased with the stimulation. Therefore, a tactile signal can impair proprioception. Moreover, there was no difference in effects of the two frequencies, which shows that both Meissner and Pacinian corpuscules are able to modulate proprioception of the ankle joint.

Finally, in their study of 2018 [46], Sacco, Gaffney and Dean applied white noise vibration to the Achilles tendon of subjects performing quiet standing and active postural positioning. They expected that the performances in these two tasks will be enhanced. Indeed, using a low-amplitude noise increases the probability that weak signals exceed a given threshold, a phenomenon called *stochastic resonance*, and therefore proprioceptive signals should be increased. The vibration was applied through C-2 tactors. Their results showed that appropriate amplitude vibration improved performances for active postural positioning but not for quiet standing.

2.2. Electrical stimulation

Electrical stimulation has also been used to induce illusory movements.

The aim of the study of Gandevia in 1985 [47] was to show the contribution of primary muscle spindle afferents to proprioception. For this purpose, electrical stimuli were delivered to the ulnar nerve of the wrist thanks to a surface electrode. The intensity of the stimulation was below the motor threshold. Subjects were seated with their arms rested on a table with the palm of the hand upwards and they did not see their hands during the experiment. The stimulation produced illusory movements of the fingers that were sensed by the subject but not visible or registered on an electromyogram. Gandevia explained these illusory movements by the perception of discharges in low-threshold muscle afferents that innervate primary muscle spindle endings. Therefore, he showed the direct contribution of Ia afferent fibres to proprioception.

In his article of 2013, Kajimoto suggested to apply electrical stimulation to muscle tendons to induce illusory movements, instead of vibration stimulation. According to him, Golgi tendon organs may be responsible of the illusory movements. Two surface electrodes were fixed on the triceps' tendons of the right arm of the subject. During the experiments, subjects

felt an illusory force pushing the right arm inward, but only some of them felt an illusory motion of the arm. However, these results were not sufficient to prove the contribution of Golgi tendon organs to the kinesthetic illusion, because muscle spindles close to the tendon might have been stimulated too.

2.3. Summary

These studies showed that vibrotactile stimulation can influence proprioception. In particular, vibrotactile stimulation can induce an illusory movement if it is applied on a tendon. Moreover, electrical stimulation can also induce an illusory movement, either by stimulating a nerve or a tendon. However, these techniques are far less explored than for vibrotactile stimulation and, to the best of our knowledge, no recent work have been done on this topic.

A comparison between all these studies is given in Table 6 on page 27.

3. Motor learning by adaptation to a perturbation

3.1. Framework

Adaptation is a form of motor learning which allows to progressively improve the execution of a motor task in presence of a perturbation that can occur in the organism or in the environment. It consists in the modification of previously learned internal models on the task. This modification is the reduction of sensory-prediction errors caused by the perturbation to return to the performances obtained under normal conditions [49].

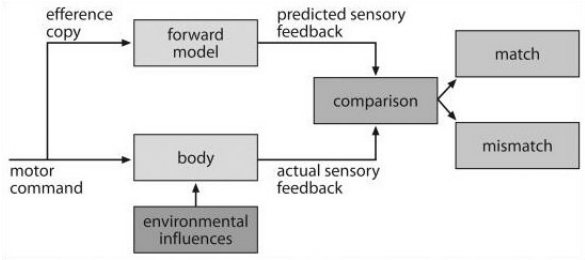

Figure 6: *Block diagram of the update processes of internal models in the central nervous system [50].*

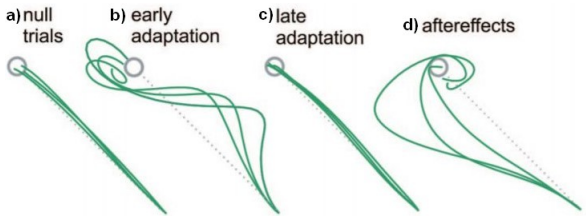

Figure 7: *Adaptation to a perturbation (b and c) and after-effects when the perturbation is suddenly stopped (d) [51].*

The functioning of internal models can be seen in Figure 6. A forward model predicts the consequences of an action and its associated sensory feedback. The real sensory feedback is compared to this predicted one. If they do not match, for example because of a perturbation, the forward model is updated to decrease progressively the error in prediction. There is therefore a new internal model created for this type of perturbation.

Table 6: *Summary of articles about the effects of a stimulation on proprioceptive feedback.*

Source	*Stimulation device*	*Stimulated area*	*Conclusions*
Vibrotactile stimulation			
Verschueren et al. 2002 [42]	Cylindrical vibrators	Hip, knee and ankle	Lengthening illusion causes the shortening of movements and proprioceptive information of one limb does not influence joint kinematics of the other limb
Albert et al. 2006 [43] Roll et al. 2009 [44]	Electromagnetic vibrators	Tendons of ankle joint	Induction of an illusory movement with patterns obtained by microneurography or via their model
Mildren and Bent 2016 [45]	Custom made pads	Foot	Tactile signal can impair proprioception
Sacco et al. 2018 [46]	C-2 tactors	Achilles tendon	Improved performances for active postural positioning but not for quiet standing
Electrotactile stimulation			
Gandevia 1985 [47]	Surface electrodes	Ulnar nerve of the wrist	Illusory movements of the fingers felt by the subject, which shows the contribution of Ia afferent fibres to proprioception
Kajimoto 2013 [48]	Surface electrodes	Triceps' tendon	Illusory force felt by the subject but not sufficient to prove the contribution of Golgi tendon organs

When the perturbation is suddenly stopped, distortion of the movements in opposite direction of the perturbation appears, called an *after-effect* (Figure 7). Then the CNS switches with another internal model and the movement becomes correct again [49].

To observe this adaptation to a perturbation, a lot of studies have been done, based either on mechanical perturbation or on visuomotor perturbation. The first type is illustrated by an experiment of Shadmehr and Brashers-Kug [52]. Subjects had to reach a target with their hand holding the handle of a robot manipulandum while a force was applied by the robot to deviate the arm of the subjects. The second type of perturbation is illustrated by the study of Martin and colleagues [53]. Subjects wore wedge prism spectacles that rotated the visual field and had to throw balls at a target.

This type of motor learning had already been investigated to restore gait pattern in several diseases using a mechanical perturbation. Indeed, patients learned new motor skills or adapt existing patterns in response to an external perturbation [54].
For **stroke** patients, a training using split-belt treadmill walking had been developed to enhance symmetric gait pattern [55, 56, 54]. The belt ran at different speeds to increase the gait asymmetry and therefore the after-effect produced a reduced gait asymmetry. By repeating this training, long-term improvements can be observed.
This same training was tested on patients with **Parkinson's disease** [57]. In addition, another type of perturbation had been tested to improve gait stability in patients suffering from this disease. They wore a pelvic belt attached to cables that can apply perturbing forces [58].
In order to study adaptive locomotor control in patients suffering from **incomplete spinal cord injury**, an experiment used the exoskeleton Lokomat to apply a resistance force on one hip [59]. After-effects induced in patients were different compared to those in controls, which suggests the use of different locomotor strategies.

3.2. Perturbation in lower-limb amputees

As it has shown good results in several diseases, mechanical perturbations have also been tested on LLA to improve their gait pattern.

To decrease the risk of falling in transtibial amputees, Kaufman and colleagues [60] assessed in 2014 the effectiveness of a falls prevention training program. This one used a treadmill and consisted in three bidirectional perturbations: (1) static perturbation, where subjects had to avoid falling when the belt suddenly moves while subject is standing, (2) static walk, where the subject had to continue walking after the initial recovery step provoked by static perturbation and (3) e-trip perturbation where it was applied randomly while the subject was walking. The training consisted of six 30 min training sessions during two

weeks, throughout the treadmill belt acceleration was increased. This study showed that subjects learned to better control their trunk thanks to the training, which is associated with reduced risk of falling. Therefore, subjects acquired a new motor skill.

Sheehan and colleagues [61] studied in 2016 the effect of gait training with surface angle perturbations on improving mediolateral walking stability in transfemoral amputees. The subjects had to follow two training sessions a week during four weeks, during which continuous walking surface angle perturbations were applied. This experiment resulted in improved walking stability, that remained five weeks later. This is because the patient had to develop skills and strategies to respond to unexpected perturbations since he cannot rely on anticipation.

As the benefit of rehabilitation training using a split-belt treadmill has been shown on gait symmetry in patients suffering from several diseases (see previous section), it has also been applied to lower-limb amputees. In their 2016 study, Kanappe and Herr [62] investigated sensorimotor learning during gait adaptation imposed by a split-belt treadmill where the belt under the prosthetic leg ran twice faster than the belt under the healthy leg. Their results confirmed that there is a sensorimotor learning showed by the after-effect observed when the perturbation was stopped. Indeed, subjects did not immediately return to baseline gait characteristics when the two belts ran at the same speed. Moreover, there was an improvement in gait symmetry in lower-limb amputees after the adaptation.

Another study aiming at investigating the effect of split-belt treadmill training on gait symmetry was performed by Kim and colleagues in 2017 [63]. The subjects followed training sessions three times a week during two weeks. This study confirmed that gait symmetry is improved after training and that it remained after one month.

3.3. Summary

Adaptation to a perturbation is a form of motor learning used in order to restore gait pattern in a number of diseases. Studies performed on LLA showed that patients acquired new motor skills and strategies to respond to unexpected perturbations in a controlled environment. The study of Sheehan and coworkers as well as the one of Kim and colleagues also showed that these strategies could be used in everyday life since they remained a few weeks after the training [61, 63].

Table 7 on page 31 compares these motor learning experiments in LLA.

Table 7: *Summary of motor learning experiments by adaptation to a perturbation in lower-limb amputees.*

Source	*Goal*	*Perturbation*	*Conclusions*
Kaufman et al. 2014 [60]	Decrease the risk of falling	Bidirectional acceleration of a treadmill belt	Acquisition of a new motor skill, trunk control
Sheehan et al. 2016 [61]	Improve walking mediolateral stability	Continuous walking surface angle perturbation	Improvement of mediolateral stability that remains after five weeks
Kannape and Herr 2016 [62]	Investigate sensorimotor learning during gait adaptation	Split-belt treadmill	Sensorimotor learning and improved gait symmetry
Kim et al. 2017 [63]	Identify effects of training on gait symmetry	Split-belt treadmill	Improvement of gait symmetry after training and retention after one month

Chapter 3

Materials and methods

As a reminder, the aim of this thesis is to investigate if an artificial sensory feedback and/or a perturbation introduced into this feedback can modify the gait pattern of able-bodied subjects. A vibrotactile stimulation of the patellar tendon of the knee is used, in continuity with the thesis of Isabelle de Thysebaert [3].
In this chapter, the characteristics of the vibrotactile stimulation used will be firstly described, chosen based on the articles of the literature review. Then, the perturbations introduced in the artificial sensory feedback are explained, as well as their expected effects on the gait pattern. It is followed by the materials used for the experiments and the experimental protocol. Thereafter, the processes to collect the data and to activate the stimulation will be explained. Finally, the tools for data processing and statistical analysis will be described.

1. Characterization of the stimulation

As explained in Section 2.1 in Chapter 2 (page 23), muscle tendon vibration can induce an illusory movement by stimulating Ia afferent fibres [42, 43]. This phenomenon can be used to provide an artificial sensory feedback to subjects for our experiments.

Artificial sensory feedback can be provided using two approaches: natural or substitutive. The first one transmits proprioceptive and tactile information of the lost limb by directly stimulating the nervous system. The second one transmits these information by using a different sensory modality, like the visual, auditory or tactile systems [32]. Using muscle tendon vibration to provide an artificial sensory feedback can be related to the natural approach, since it stimulates the Ia afferent fibres which is a type of sensory nerves.

1.1. Stimulated area

As the stimulation is chosen to be non-invasive, it has to be applied on an easily accessible tendon. This is why the patellar tendon of the knee is chosen. Therefore, this stimulation could be used in transtibial amputees.

The patellar tendon is actually a ligament as it connects the bottom part of the patella with the top part of the tibia (Figure 8). It belongs to the extensor mechanism, composed of the quadriceps muscle, the quadriceps tendon, the patella and the patellar tendon. They play a role in knee extension as they straighten this joint [65].

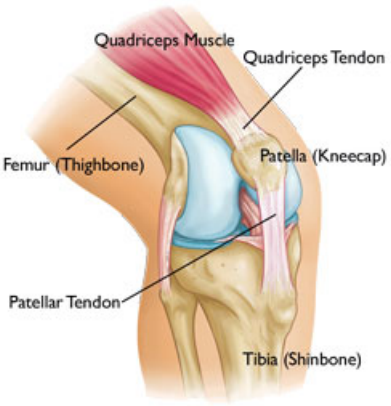

Figure 8: *Anatomy of the patellar tendon [64].*

The knee stability is ensured by proprioceptive inputs from mechanoreceptors located in tendons, ligaments and muscles surrounding it. Most of them are free nerves endings, *i.e.* pain receptors, Ruffini corpuscles and Golgi tendon organs [66], which were explained in Section 2.1 in Chapter 1 (page 4).

1.2. Stimulation characteristics

Several studies used the illusory movement induced by muscle tendon vibration, which is believed to be due to the stimulation of Ia afferent fibres [43, 44, 42]. In actual movements, the natural firing rates of these fibres are between 10 and 30 Hz. However, to induce the illusion of movement, frequency between 80-100 Hz must be used [43]. As the majority of articles studying the induction of illusory movements used a 80 Hz vibration stimulation [43, 44], this is the frequency that will be used for this experiment. This should provide an artificial sensory input to the CNS.

Moreover, a discrete stimulation is used, *i.e* which is applied at a given time and not all along the knee movement. Indeed, as mentioned in the literature review (see Section 1.3 of Chapter 2 on page 15), the human brain can more easily process and incorporate time-discrete somatosensory information in its internal models, without adding cognitive load [9]. The duration of the stimulation is 100 ms, which is long enough for the CNS of subjects to perceive it.

Ia afferent fibres transmit sensory information when the muscle is lengthened [67]. Therefore, the discrete stimulation has to be applied on the tendon connected to this muscle when it is stretched, *i.e.* at the maximum knee flexion. This occurs approximately at 73% of the gait cycle [68].

The stimulation characteristics are therefore the following:

- Frequency: 80 Hz;
- Duration: 100 ms;
- Phasing: maximum knee flexion;
- Discrete stimulation.

2. Perturbation of artificial sensory feedback

As previously explained, one of the objectives of this work is to study the effects of a perturbation introduced in the artificial sensory feedback on the gait pattern of able-bodied subjects. This perturbation consists in the introduction of an offset in the delivering time of the stimulation:

- The stimulation is applied 5% of the gait cycle before the maximum knee flexion.
- The stimulation is applied 5% of the gait cycle after the maximum knee flexion.

An offset of 5% is chosen because it is short enough for subjects to not detect it. In this way, the stimulation and the perturbation are unconscious.

We hypothesize that the three stimulation conditions (at maximum knee flexion, with a negative offset and with a positive offset) should influence the spatio-temporal parameters of the gait pattern.
Firstly, when the stimulation is applied at the maximum knee flexion, we expect to observe that the subject will not complete his movement, since his tendon feels like it is more lengthened than it really is. This should only be observed in the spatial parameters of the gait pattern, *i.e.* the amplitude of the knee movement. In contrast, we should not observe any effect on the temporal parameters of the gait pattern (phase lead between legs and stride duration) compared to the case where there is no stimulation, since the stimulus is applied without any delay with respect to the maximum knee flexion.
Secondly, when the stimulation is applied 5% of the gait cycle before this event, we expect that the subject will conclude his movement earlier than when there is no stimulation, because the tendon feels like it is lengthened before it really is. Therefore, it should also lead to a change in the temporal parameters, since the stimulated leg finishes its movement earlier than in the case where there is no stimulation applied.

Finally, when the stimulation is applied 5% of the gait cycle after the maximum knee flexion, we expect that the movement of the stimulated leg will be extended, since the tendon feels like it is lengthened while it was starting to shorten. Therefore, we also expect a change in temporal parameters, since this time the stimulated leg finishes its movement later than in the case where there is no stimulation applied.

3. Materials

Eight able-bodied subjects participated in the experiments (six females), which were 23.3 ± 1.7 year old, except one subject that was 54 year old. In order to measure gait trajectories, Inertial Measurement Units (IMUs, Figure 9) were placed on the right and left shanks of the subject in the orientation given in Figure 10. IMUs contain three-axis gyroscope, accelerometer and magnetometer. This work only analysed the accelerations and angular velocities provided by the accelerometer and the gyroscope respectively, since they are the more relevant to study gait parameters. IMUs were connected to a Lenovo Yoga 720 computer by Bluetooth. The sampling frequency was 128 Hz. The open source C# code provided by x-io Technologies [69] was modified in order to activate the vibrotactile stimulation at the desired time, as explained in the following sections.

Figure 9: *x-IMU, x-io Technologies Limited (United Kingdom) [70].*

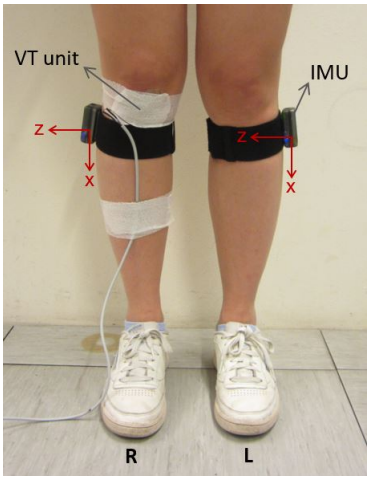

Figure 10: *Layout of the vibrotactile (VT) unit and the IMU on the right and left legs of the subject.*

The vibrotactile stimulus was delivered through a high-bandwidth vibrotactile transducer, also known as "haptuator". The planar version of the original haptuator from Tactile Labs (Montreal, Canada) was used [71], which is more suitable for skin stimulation (Figure 11a). It is a recoil-type vibrotactile actuator. It is composed of a cylindrical permanent magnet suspended by two rubber membranes via two non-ferromagnetic pins inside a tubular

enclosure and a coil wrapped around the enclosure (Figure 11b). Therefore, when there is a current inside the coil, it creates a Laplace force in the axial direction by interacting with the magnetic field of the magnet. This force moves the magnet axially, making the haptuator vibrating [72].
The vibrotactile unit was placed on the right patellar tendon of the subject thanks to a self-adhesive tape, and the wire connecting it to the computer was secured in order to not pull on the haptuator (Figure 10).

For the experiment, the subject had to walk on a treadmill at 4 km/h during 5 min.

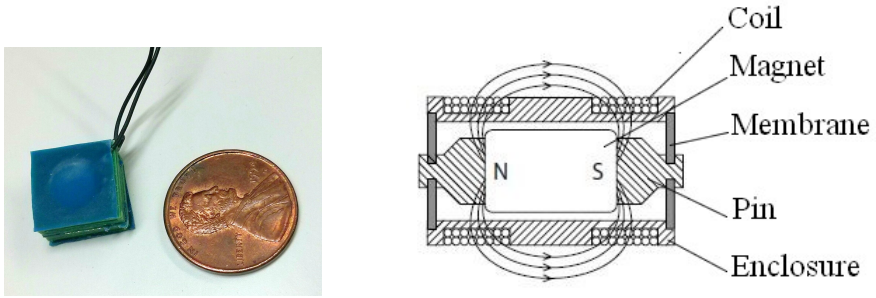

(a) **(b)**

Figure 11: *(a) External design of the vibrotactile unit, Haptuator Planar, Tactile Labs (Montreal, Canada) [71]; (b) Internal design [72].*

4. Data collection and stimulation activation

The IMU signal chosen to determine when to activate the stimulation is the one of the gyroscope in the z-direction which corresponds to the shank angular velocity, one of the most used signals for heel strike detection. This signal is processed in order to apply the vibrotactile stimulation at the maximum knee flexion or with a specific offset with respect to this event. For this, a gait phase estimator like the one described by Yan and colleagues [73] is used. It is composed of three main parts (Figure 12): an event detector, a gait phase estimator based on adaptive oscillators and a phase error compensator. These three subsystems are detailed in this section.

4.1. Signal learning

The goal of this subsystem is to obtain an estimate of a continuous phase variable $\varphi(t)$ by learning from a biomechanical signal $\theta(t)$. Since our input signal, *i.e* the shank angular velocity, is periodic, this can be done with adaptive oscillators (AOs).

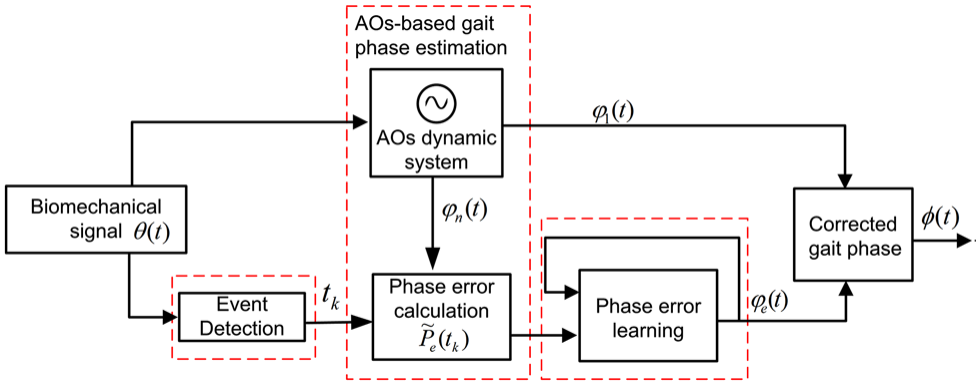

Figure 12: *Block diagram of the gait phase estimator. The biomechanical signal passes through the three subsystems: the event detector, the gait phase estimator based on adaptive oscillators, and the phase error compensator. The output is the corrected gait phase [73].*

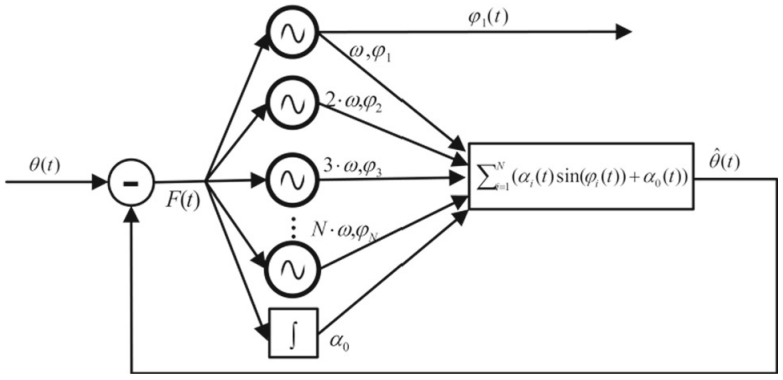

Figure 13: *Block diagram of the functioning of adaptive oscillators. The input signal is decomposed into several harmonics. Phase, frequency and amplitude of each harmonic are learned by each oscillator and then combined to obtain an estimation of the input signal [73].*

The functioning of AOs is represented in Figure 13. The input signal can be decomposed in several harmonics (here three) and therefore three AOs are used. Each oscillator learns the features of one of the harmonics i, like the fundamental frequency ω, their phase φ_i, their amplitude α_i and the offset α_0. These characteristics are learned from the error signal, *i.e.* the difference between the input signal $\theta(t)$ and its estimate $\hat{\theta}(t)$ that is fed back to the state estimates [73]:

$$F(t) = \theta(t) - \hat{\theta}(t)$$

The variations of these features are therefore given by [73]:

$$\dot{\varphi}_i(t) = \omega(t) \cdot i + \nu_\varphi \frac{F(t)}{\sum \alpha_i} \cos[\varphi_i(t)] \tag{1}$$

$$\dot{\omega}(t) = \nu_\omega \frac{F(t)}{\sum \alpha_i} \cos[\varphi_1(t)] \tag{2}$$

$$\dot{\alpha}_i(t) = \eta F(t) \sin[\varphi_i(t)] \tag{3}$$

$$\dot{\alpha}_0 = \eta F(t) \tag{4}$$

Finally, the input signal is approximated by a frequency summation of the extracted variables, that corresponds to a sort of real-time Fourier decomposition [73]:

$$\hat{\theta}(t) = \sum_{i=1}^{3} \alpha_i(t) \sin[\varphi_i(t)] + \alpha_0(t) \tag{5}$$

Numerical values of the learning gains of the oscillators (equations 1-4) were obtained from [74]:

$$\nu_\omega = \frac{20}{\tau_\omega^2}, \quad \nu_\varphi = \sqrt{24.2\nu_\omega} \quad \text{and} \quad \eta = \frac{2}{\tau_\alpha}$$

With $\tau_\omega = 0.75T$ [s] and $\tau_\alpha = T$ [s] the learning frequency and amplitude time constants respectively, with T the stride duration. With this tuning, the adaptive oscillator should converge to steady-state within approximately three cycles. Therefore, the stimulation is activated only after three gait cycles.

4.2. Gait event detection

The goal of this subsystem is to identify the beginning of a new gait cycle at time t_k. By convention, a gait cycle starts with the heel strike (see Section 2.2 in Chapter 1 on page 7), and the maximum knee flexion arises at 73% of the gait cycle (Figure 14) [68]. However, this event is difficult to detect since it is not the only minimum in the shank angular velocity signal. Instead, the maximum of the signal, corresponding to the mid swing phase, is chosen for the onset of the gait cycle. With this new cycle phase reference, the maximum knee flexion arises at 88% of the gait cycle.

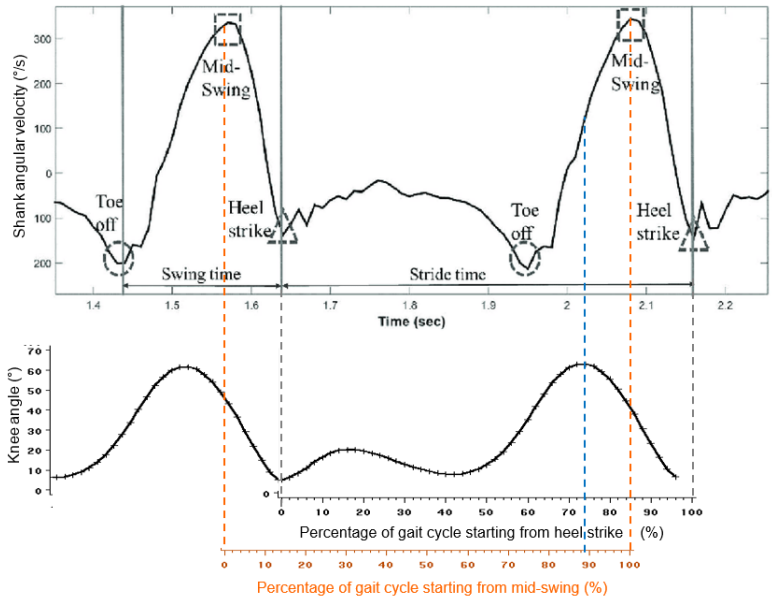

Figure 14: *Shank angular velocity (top) and knee angle (bottom) during one gait cycle, adapted from [75, 76].*

The maximum is identified if the three following conditions are met:

- The amplitude of the approximated angular velocity signal given by equation (5) is bigger than a threshold, to avoid local maxima detection:

$$\hat{\theta} > 150$$

- The point corresponds to a maximum:

$$\hat{\theta}_{i-1} < \hat{\theta}_i \quad \text{and} \quad \hat{\theta}_{i+1} < \hat{\theta}_i$$

- The elapsed time since the last mid swing is larger than a significant fraction of the previous cycle duration [73]:

$$t^* - t_k \geq \rho \frac{2\pi}{\omega(t^*)}$$

  Where t^* is the possible new time at which a maximum is detected, t_k is the previous time where it occurred, ω is the fundamental frequency of the signal and $\rho < 1$ is a gain tuning the minimum time interval before detection of a new contact time.

The approximated angular velocity signal $\hat{\theta}(t)$ provided by the AOs is used because it is smoother than the raw signal. Therefore, it facilitates the detection of maxima, that is polluted by noise in the raw signal, without adding a delay due to filtering.

4.3. Gait phase estimation and stimulation activation

The gait phase should linearly increase from 0 to 100% between two mid swing detections. Firstly, the learned fundamental phase $\varphi_1(t)$ is normalized between 0 and 2π [73]:

$$\varphi_n(t) = \text{mod}(\varphi_1(t), 2\pi)$$

Secondly, in order to have φ_n equal to 0 rad at time t_k when a mid swing is detected, a phase error $P_e(t_k)$ is defined as the error between the learned phase $\varphi_n(t)$ at time t_k and 0 or 2π [73]:

$$P_e(t_k) = \begin{cases} -\varphi_n(t_k) & \text{if } 0 \leq \varphi_n(t_k) < \pi \\ 2\pi - \varphi_n(t_k) & \text{if } \pi \leq \phi_n(t_k) < 2\pi \end{cases}$$

To avoid inconsistencies when $\varphi_n(t_k)$ fluctuates around π rad, the phase error is corrected [73]:

$$\tilde{P}_e(t_k) = \begin{cases} P_e(t_k) - 2\pi & \text{if } P_e(t_k) > \pi/2 \text{ and } \tilde{P}_e(t_{k-1}) < -\pi/2 \\ P_e(t_k) + 2\pi & \text{if } P_e(t_k) < -\pi/2 \text{ and } \tilde{P}_e(t_{k-1}) > \pi/2 \\ P_e(t_k) & \text{otherwise} \end{cases}$$

Thirdly, in order to avoid an abrupt change in the gait phase at each mid swing detection, a new variable $\varphi_e(t)$ is used to filter $\tilde{P}_e(t_k)$ within one stride [73]:

$$\dot{\varphi}_e = \varepsilon(t_k)\omega e^{-\omega(t-t_k)}$$

With $\varepsilon(t_k) = k_p[\tilde{P}_e(t_k) - \varphi_e(t_k)]$ the value capturing the desired variation of $\varphi_e(t)$ and k_p a proportional gain which is set to 0.3 in this work.

Finally, the gait phase is given by

$$\phi(t) = \text{mod}(\varphi_n(t) + \varphi_e(t), 2\pi) \tag{6}$$

This value is divided by 2π to obtain a gait phase varying between 0 and 1. This signal can be observed in Figure 15. It can already be noticed that this gait phase signal is not really accurate, as it does not start at 0 exactly at the event detection.

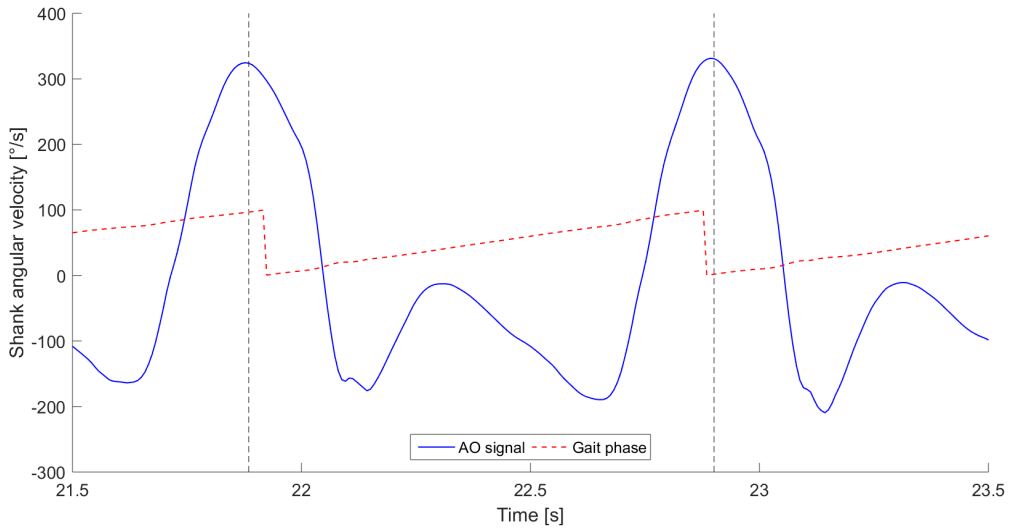

Figure 15: *Evolution of the gait phase signal $\phi(t)$ (multiplied by 100) between two mid swing detections, indicated by vertical dashed lines (based on data from [3]).*

Therefore, there are two conditions to activate the vibration:

- The condition given by equation (6):

$$\phi(t) > 0.88$$

  This condition is modified depending on the experimental condition, *i.e.* 0.93 and 0.83 for the positive offset and the negative offset respectively.

- A time condition on the minimum time interval since the last stimulation:

$$t - t_v \geq \rho \frac{2\pi}{\omega(t)}$$

  It ensures that the stimulation is activated only once when the gait phase exceeds 88%.

4.4. Hardware delay quantification

There is a delay between the time where the vibration is activated in the code and the time of the actual vibration, which is due to execution time of the code by the computer. A C# code was created to activate the vibrotactile unit every 10 seconds. In order to determine when the vibrotactile unit actually vibrates, it is placed on top of an IMU, and they are fixed together on a stable surface (Figure 16). Then, the acceleration signal in the z-direction from the IMU is analysed in Matlab. Every peak corresponds to a vibration (Figure 17).

The hardware delay is computed by making the difference between the vibration time and the activation time. The mean delay is equal to 0.17 s with a variance of 0.0423 s. This

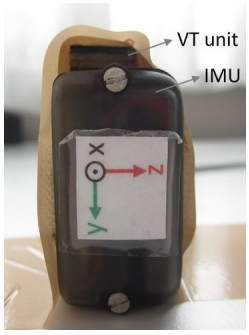

Figure 16: *Layout of the vibrotactile (VT) unit on the IMU, fixed together on a table.*

is quite variable. However, the maximum value for the delay corresponds to 0.33 s for the first stimulation, which can be due to the launching of the code. If this event is not taken into account, the mean delay is 0.16 s with a standard variation of 0.015 s, which is much more acceptable.

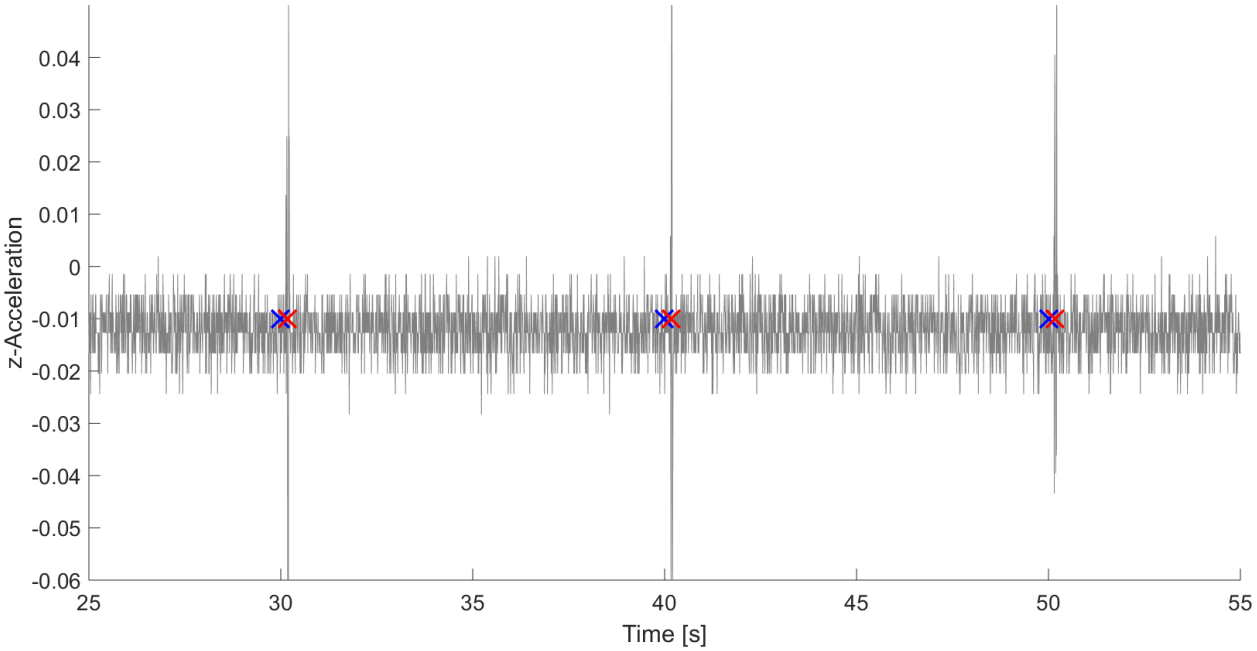

Figure 17: *Acceleration signal in the z-direction from the IMU, with blue crosses corresponding to activation times and red crosses to stimulation times.*

This delay is taken into account in the C# by adding the term ωt_{delay} to equation (6) and is shown in Figure 18:

$$\phi_{delay}(t) = \mathrm{mod}(\varphi_n(t) + \varphi_e(t) + \omega t_{delay}, 2\pi)$$

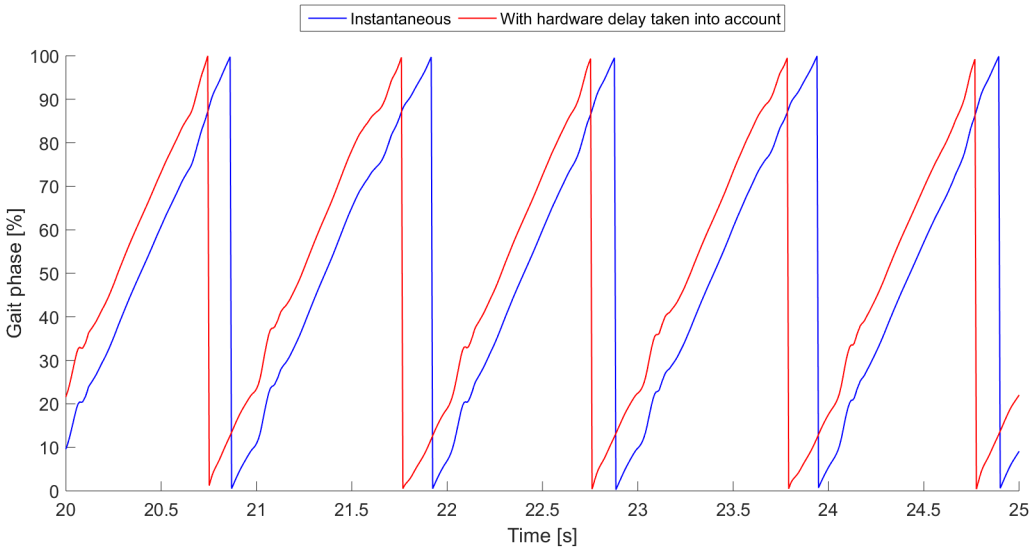

Figure 18: *Instantaneous gait phase signal in blue and with the hardware delay taken into account in red (based on data from [3]).*

4.5. Experimental protocol

The experiment was composed of several steps.

4.5.1. Verification of the parameters

This step allows to observe if the C# code activates the stimulation at the right time. For this, the subject walks on the treadmill at 4 km/h with an IMU placed on his right shank.

The C# code provided by x-io Technologies [69] has been modified to display in red the signal from the AOs (see Section 4.1 on page 37), in blue the detected maxima, and in green the times where the stimulation is activated (Figure 19). This allows to determine if the maximum is detected every time. If this is not the case, some parameters have to be decreased: the parameter ρ, which tunes the minimum time interval before detection of a new contact time, and the amplitude of the mid swing. The default values of these parameters are 0.5 and 150 respectively. For this work, it turned out that it was not necessary to change them because the maxima were correctly detected each time.

4.5.2. Experiment

The experiment is decomposed into four experimental conditions. For all of them, the subject walks on the treadmill at 4 km/h during 5 min. The vibrotactile unit is placed on the right patellar tendon only for the last three conditions.

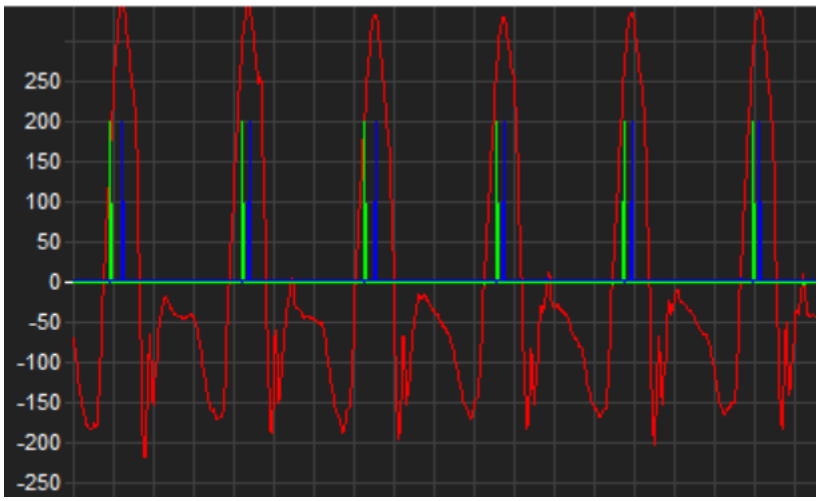

Figure 19: *Real-time monitoring of the most relevant signals during parameters verification, with in red the shank angular velocity signal around the z-axis learned by the adaptive oscillators, in blue the maxima detected and in green the times where the stimulation is applied.*

The different experimental conditions are:

- Without vibration: no vibration is activated.
- No offset: the vibration is activated at 88% of the gait cycle.
- Negative offset: an offset of 5% of the gait cycle is subtracted to the vibration's activation time, *i.e.* the vibration is activated at 83% of the gait cycle.
- Positive offset: an offset of 5% of the gait cycle is added to the vibration's activation time, *i.e.* the vibration is activated at 93% of the gait cycle.

These two lasts conditions are randomized between subjects.

5. Data processing

Once the experiments have been conducted, IMUs signals are processed off-line to remove the noise in order to extract interesting parameters for the statistical analysis.

5.1. Signals of interest

Only three signals from the IMUs are used, all of them being in the sagittal plane (Figure 20):

a) The angular velocity around the z-axis: rate at which the shank angular position changes;

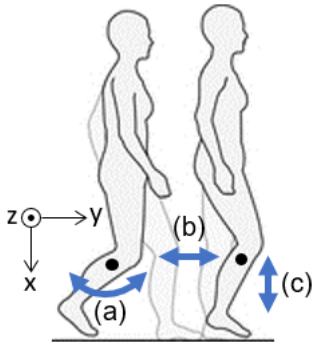

Figure 20: *Displacements of the shank during a gait cycle, adapted from [14].*

b) The horizontal acceleration (y-axis): acceleration of the anterior and posterior displacements of the shank;

c) The vertical acceleration (x-axis): acceleration of the up and down displacements of the shank.

The angular velocity is used to segment all the other signals into strides. The segmentation goes to one mid swing phase to the next one, which corresponds to a maximum in the shank angular velocity signal. For the signals of the left leg, they are segmented based on the segmentation of the right leg. Several variables are computed to be analysed by the statistical tools:

- The stride duration is calculated by making the difference between two successive times corresponding to a maximum of the angular velocity;
- The phase lead between the legs corresponds to the time where the maximum appears in the left angular velocity signal;
- The amplitude of the signal is also analysed. Depending on the signal (see Chapter 4 on page 51), it is either the peak-to-peak amplitude, *i.e.* the amplitude from the minimum to the maximum of the signal, or the amplitude of the maximum following the stimulation that is analysed;
- The occurrence time of the maximum after the stimulation for the three signals is also analysed, in order to establish if the stimulation offset induced a temporal distortion in the gait pattern.

5.2. Signal processing

The IMU signals are filtered with a 2nd order Butterworth low-pass filter with a cut-off frequency of 5 Hz. The discrete-time system function for this filter is given by the following equation [77].

$$x'[i] = a_0 x[i] + a_1 x[i-1] + a_2 x[i-2] - b_1 x'[i-1] - b_2 x'[i-2]$$

With $x[i]$ the input time series of the filter and $x'[i]$ the output time series. The coefficients are given by [77]:

$$\Omega_c = \tan(\pi \frac{f_c}{f_s})$$

$$c = 1 + \sqrt{2}\Omega_c + \Omega_c^2$$

$$a_0 = a_2 = \frac{\Omega_c^2}{c}$$

$$a_1 = 2a_0$$

$$b_1 = \frac{2(\Omega_c^2 - 1)}{c}$$

$$b_2 = \frac{1 - \sqrt{2}\Omega_c^2 + \Omega_c^2}{c}$$

With f_c the cut-off frequency and f_s the sampling frequency, which is 128 Hz. The results of this filtering are shown in Figure 21.

After being filtered, the signals are segmented into strides as previously explained. Thereafter, each stride is interpolated on 100 points which are then averaged within subjects. The variables on which the statistical analysis is performed are obtained from gait cycle signals for each subject. The graphs shown in Chapter 4 correspond to the averaged signals of one gait cycle between subjects.

6. Statistical analysis

The statistical analysis is performed in R. The tool used for our data is a repeated measures ANOVA, because in the experiments, the same subjects are being measured several times on the same variables [78]. It allows to compare the means between the different stimulation conditions and between the legs. Either one-way or two-way repeated measures ANOVA can be used, depending on the variable being analysed. Before applying those tests, the assumptions of the repeated-measures ANOVA have to be verified. They can be found in Appendix A on page 71.

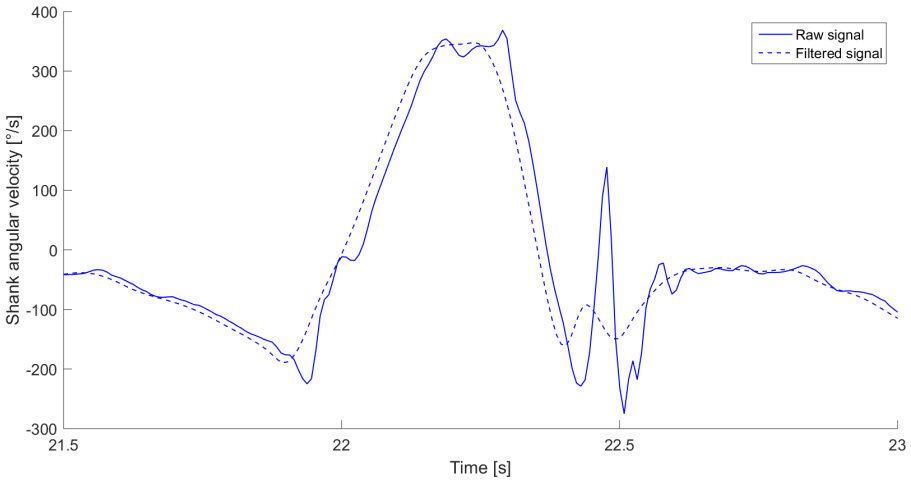

(a)

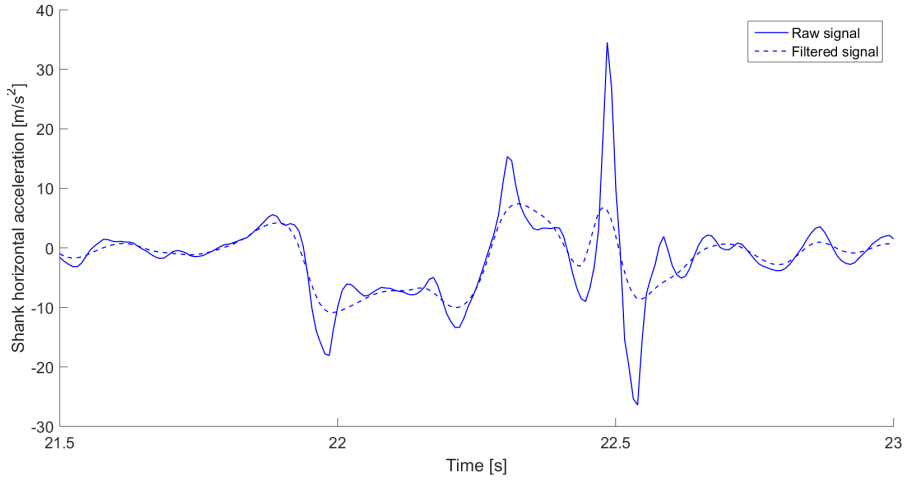

(b)

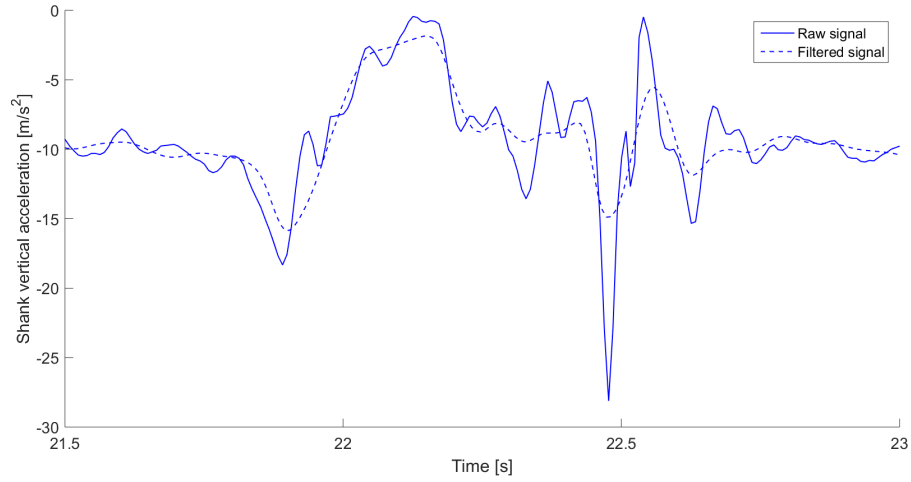

(c)

Figure 21: *Graph of raw signals (solid line) and of filtered signals (dashed line) for (a) the angular velocity, (b) the horizontal acceleration and (c) the vertical acceleration. Signals are these of the right leg of the first subject for the condition where there is no stimulation applied.*

In R, the repeated measures ANOVA is associated with a Mauchly's test for sphericity, which is an assumption of this test (see Section A.2 in Appendix A on page 71). When this condition is violated, two corrections can be applied: the Greenhouse-Geisser (GG) correction and the Huynd-Feldt (HF) correction. Therefore, when one of these corrections is used, it is indicated by its corresponding initials given just after the p-value.

If there is any significant difference between the means of the four experimental conditions, a pairwise t-test is used to apply a t-test on each combination of conditions [79]. This allows to determine between which conditions the means are significantly different. The p-value for the pair of conditions where there is no stimulation applied and where the stimulation is applied at maximum knee flexion allows to determine if vibration only can influence the gait pattern. Moreover, the p-values for the pairs of conditions where the stimulation is applied without any offset compared to those applied either with a negative or a positive offset allow to analyse if this perturbation introduced in the stimulation influences the gait pattern of subjects.

6.1. One-way repeated measures ANOVA

This test analyses the effects of one factor, which in our case is the experimental conditions (no stimulation, stimulation with no offset, stimulation with a negative offset and stimulation with a positive offset). Its hypotheses are given by [80, 78]:

$$\begin{cases} H_0 : & \mu_1 = \mu_2 = \mu_3 = \mu_4 \\ H_a : & \text{at least two means are significantly different} \end{cases}$$

With μ_1, μ_2, μ_3 and μ_4 the means of the four conditions for the stimulated (right) or for the non-stimulated (left) leg.

This test is applied on the phase lead between the legs. It is also applied on the occurrence times of the maximum just after the stimulation, distinctly for the right and left legs [79].

6.2. Two-way repeated measures ANOVA

This test allows to determine the effects of two factors and of their interaction on the variables. In our case, these factors are the legs and the four stimulation conditions. The hypotheses of this test are given by [80]:

$$\begin{cases} H_{01} : & \mu_{1,1} = \mu_{1,2} \\ H_{a1} : & \mu_{1,1} \neq \mu_{1,2} \end{cases}$$

With $\mu_{1,\bullet}$ the mean of the factor corresponding to the legs.

$$\begin{cases} H_{02}: & \mu_{2,1} = \mu_{2,2} = \mu_{2,3} = \mu_{2,4} \\ H_{a2}: & \text{at least two means for the second factor are significantly different} \end{cases}$$

With $\mu_{2,\bullet}$ the mean of the factor corresponding to the experimental conditions.

$$\begin{cases} H_{03}: & \text{there is no interaction between both factors} \\ H_{a3}: & \text{there is an interaction between both factors} \end{cases}$$

This analysis is applied on the stride durations and on the amplitudes of the angular velocity and acceleration signals [81].

6.3. Pairwise t-test

A pairwise t-test is a t-test performed on each pair of experimental conditions. In our case, a paired t-test is used, because the different experimental conditions are performed on the same subjects. Its hypotheses are [82]:

$$\begin{cases} H_0: & \mu_1 - \mu_2 = 0 \\ H_a: & \mu_1 - \mu_2 \neq 0 \end{cases}$$

With μ_1 and μ_2 the means of the two conditions being compared.

7. Summary

There are four experimental conditions: (1) no vibration applied, (2) the vibration is applied at the maximum knee flexion, (2) the vibration is applied with an offset of 5% before this event and (4) after this event. Three signals will be used for the statistical analysis: the angular velocity around the z-axis, the horizontal acceleration and the vertical acceleration of the right and left shanks.

The following chapter will describe the results obtained thanks to the statistical tools explained in this chapter. A one-way and two-way repeated measures ANOVA are applied on several variables: stride duration, phase lead between the legs, occurrence time of the maximum amplitude after the stimulation and amplitude for the three signals.

Chapter 4

Results

In this chapter, the results of the several tests explained in the previous chapter are shown. Firstly, the shank angular velocity is used to analyse the stride durations and the phase leads between the legs for each condition. The amplitude of the maximum of this signal just after the stimulation is also studied. Then, the peak-to-peak amplitude of the shank horizontal acceleration is analysed, as well as the occurrence time of the first maximum just after the stimulation for this signal. Finally, these same variables are also studied for the shank vertical acceleration.

Before testing these elements, the assumption of normality is firstly checked for all the data (see Section A.3 in Appendix A on page 71). For all the following statistical tests, if the p-value is lower than a significant level $\alpha = 0.05$, the null hypothesis can be rejected.

1. Shank angular velocity

1.1. Stride duration

The two-way repeated measures ANOVA on the stride durations gives the following p-values: 0.8 (GG) for the effects of the experimental conditions only, 0.122 for the effects of legs only, and 0.53 (GG) for the effects of the interaction of both factors. Therefore, the null hypothesis according to which means are equal cannot be rejected, and there is no effect of the interaction between legs and conditions. Indeed, it can be observed in Figure 22 that in all conditions, the stride duration was about 1.16 s, thus corresponding to a gait cadence of 0.86 Hz.

1.2. Phase lead between legs

The one-way repeated measures ANOVA on the phase leads between the legs gives a p-value of 0.252 (GG). Therefore, the hypothesis where the means between the experimental conditions are equal cannot be rejected. Figure 23 shows that there is effectively almost no

variation between the means of the phase leads between the different experimental conditions. Indeed, the phase lead between legs is around 50% in all conditions, which corresponds to what was expected.

1.3. Amplitude

In Figure 24, it can be observed that the main difference between the signals of the shank angular velocity between the different conditions occurs at the global maximum, which follows the stimulation (*i.e.* 83, 88 or 93% of the gait cycle, depending on the experimental condition). Therefore, a two-way repeated measures ANOVA is applied on this variable. Its results are a p-value of 0.096 (GG) for the effects of conditions only, 0.302 for the effects of legs only and 3.97×10^{-7} (HF) for the effects of the interaction of both factors. Therefore, the null hypothesis cannot be rejected for both factors independently, but there is an effect of the interaction between the factors. Figure 25 shows the differences in the means between conditions for both legs.

To determine in which pair of conditions and for which leg the means are significantly different, a pairwise t-test is completed (see Table B1 in Appendix B on page 74). The only p-value lower than the significant level is the one of the pair of conditions where there is no stimulation applied compared to the one where the stimulation is applied without any offset for the right leg (0.039). It appears that the maximum amplitude of the first condition (mean of 352 °/s) is higher than the one of the second condition (mean of 342 °/s). In contrast, the null hypothesis cannot be rejected for any pair of conditions for the left leg. In Figure 26, it can be observed that the angular velocity signal for the condition where the vibration is applied without any offset matches the one for the condition where there is no vibration applied for the right leg, except at the maximum just after the stimulation.

2. Shank horizontal acceleration

2.1. Amplitude

Figure 27 shows that there is some variation of the peak-to-peak amplitudes between the different experimental conditions. A two-way repeated measures ANOVA applied on this variable gives the following p-values: 0.120 (GG) for the effects of the experimental conditions only, 0.160 for the effects of legs only, and 0.043 (HF) for the effect of the interaction between both factors. Therefore, the null hypothesis can only be rejected for this last case. However, this p-value is just below the significant level $\alpha = 0.05$. Therefore, when applying the pairwise t-test to determine for which pairs of experimental conditions the means are significantly different, neither p-value is below this threshold (see Table B2 in Appendix B on page 75). The means of the peak-to-peak amplitudes of the horizontal acceleration are given in Figure 28.

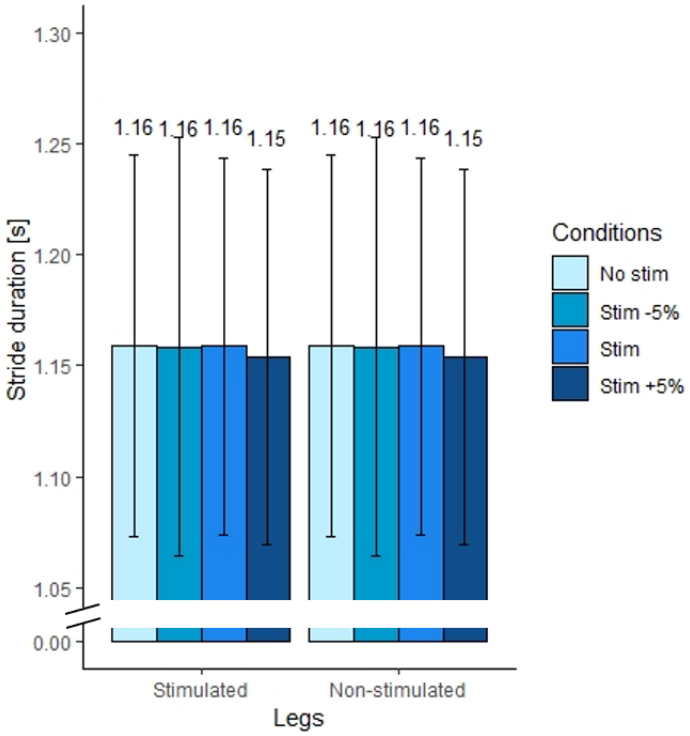

Figure 22: *Comparison of the stride durations [s] for each leg and each condition. The means are represented by the bars and the standard deviations by the vertical lines.*

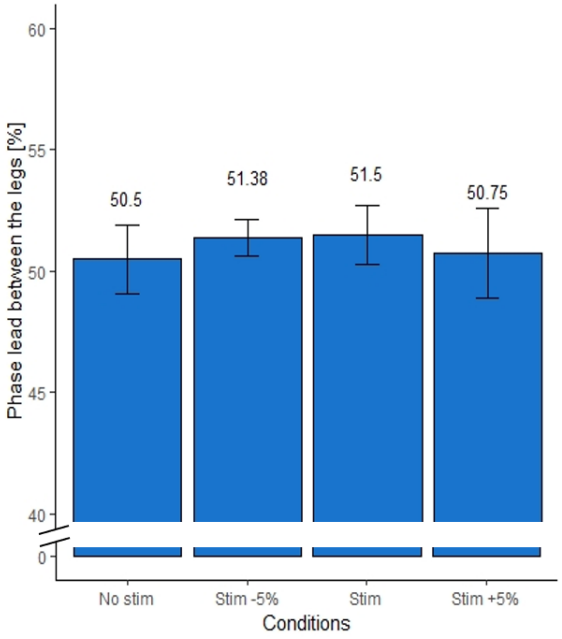

Figure 23: *Comparison of the phase leads [%] between the legs for the four experimental conditions. The means are represented by the bars and the standard deviations by the vertical lines.*

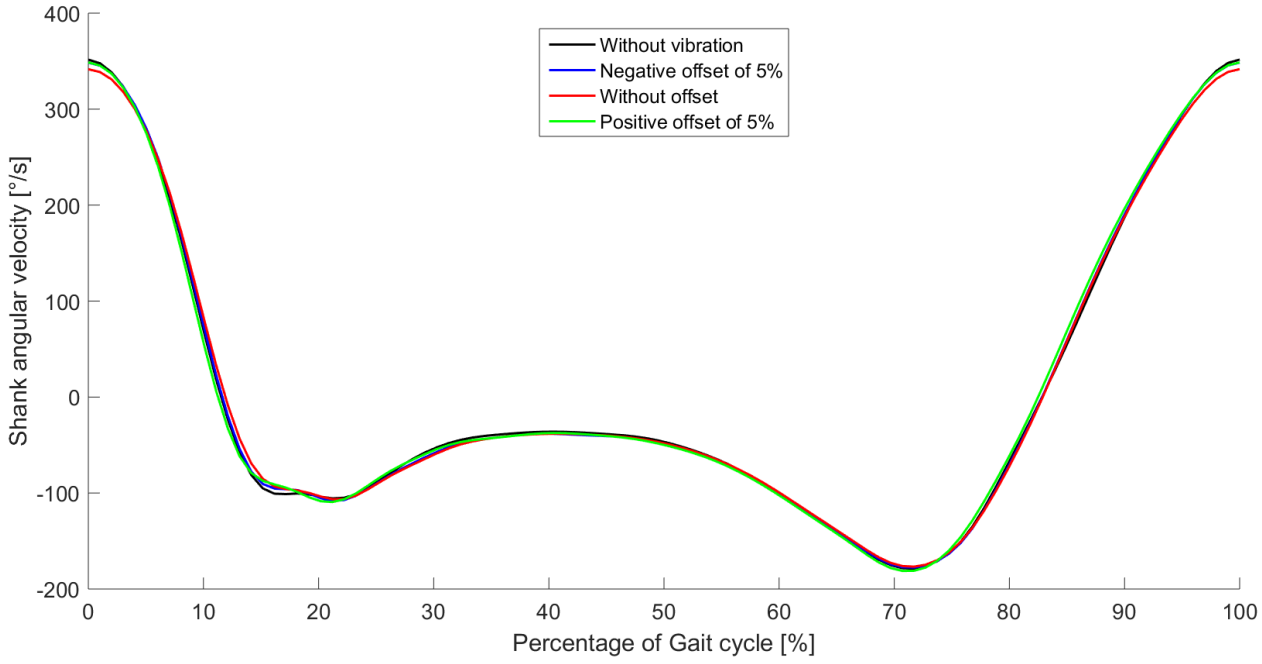

(a)

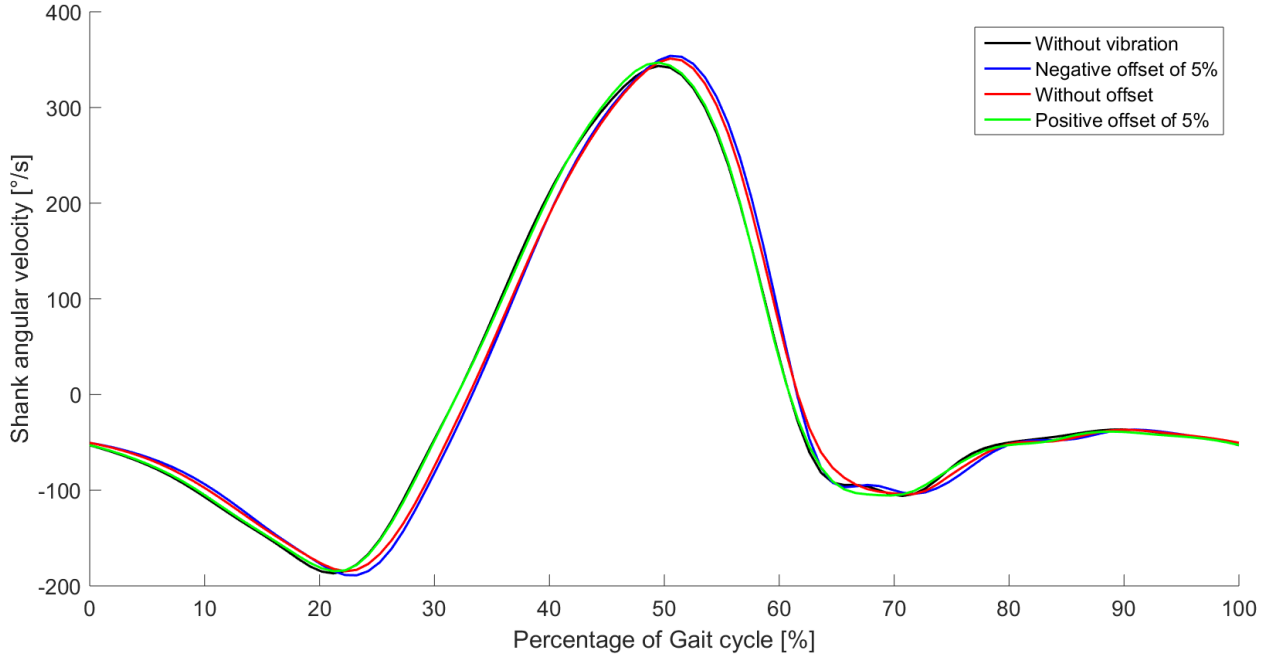

(b)

Figure 24: *Graph of the shank angular velocity [°/s] for (a) the stimulated leg and (b) the non-stimulated leg, with the condition where there is no stimulation applied in black, where the stimulation is applied with a negative offset of 5% in blue, where it is applied without any offset in red and with a positive offset of 5% in green.*

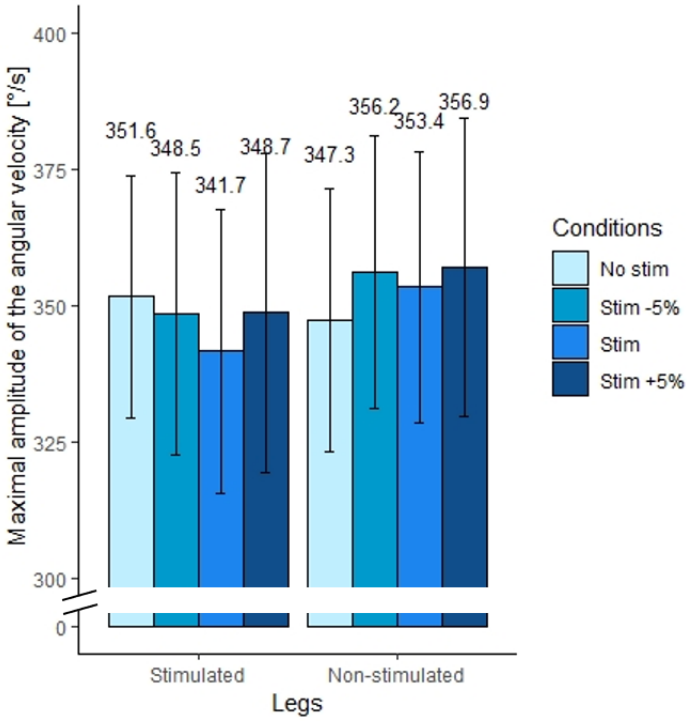

Figure 25: *Comparison of the maximum amplitudes of the shank angular velocity [°/s] for each leg and each condition. The means are represented by the bars and the standard deviations by the vertical lines.*

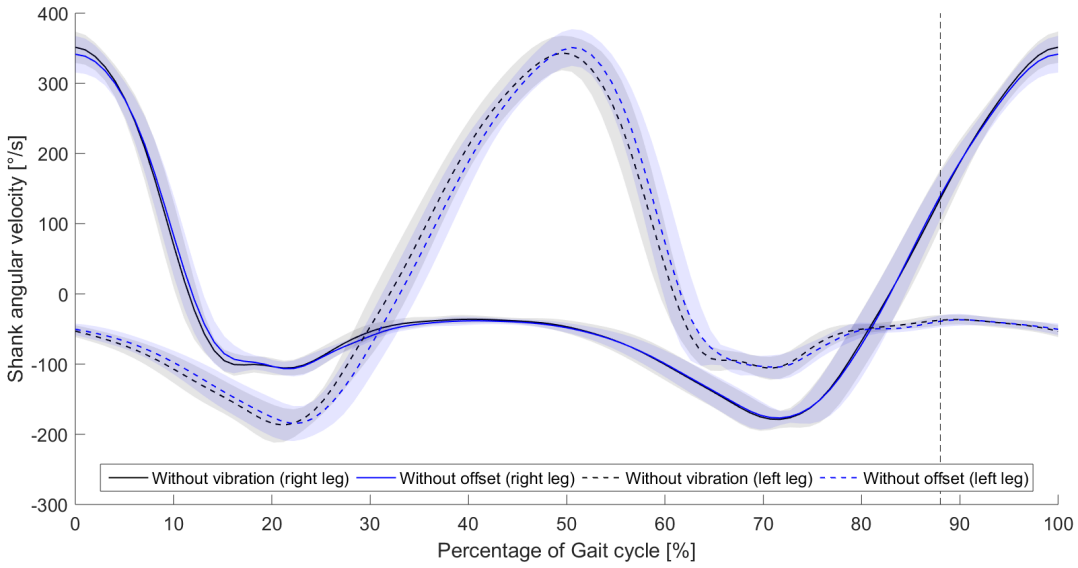

Figure 26: *Graph of the shank angular velocity [°/s] of the stimulated leg (solid line) and of the non-stimulated leg (dashed line) for the pair of conditions where there is no stimulation applied (black) and where the stimulation is applied at the maximum knee flexion (blue). The shaded area represents the standard deviation for each signal and the vertical dashed line the maximum knee flexion.*

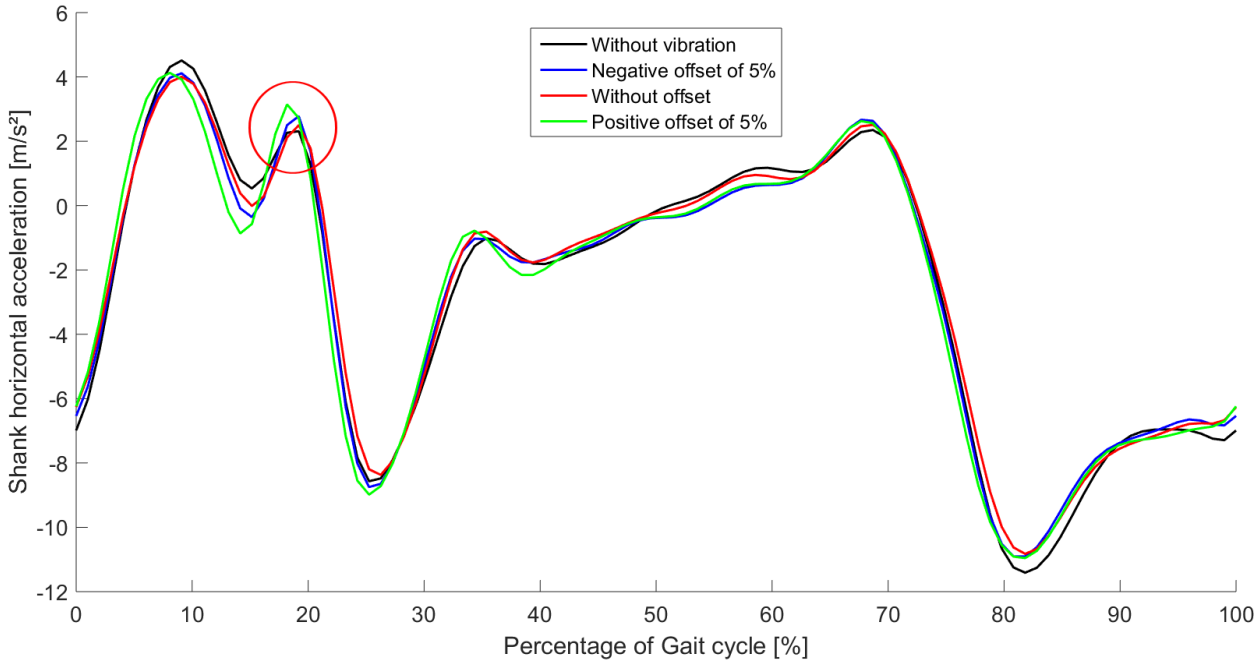

(a)

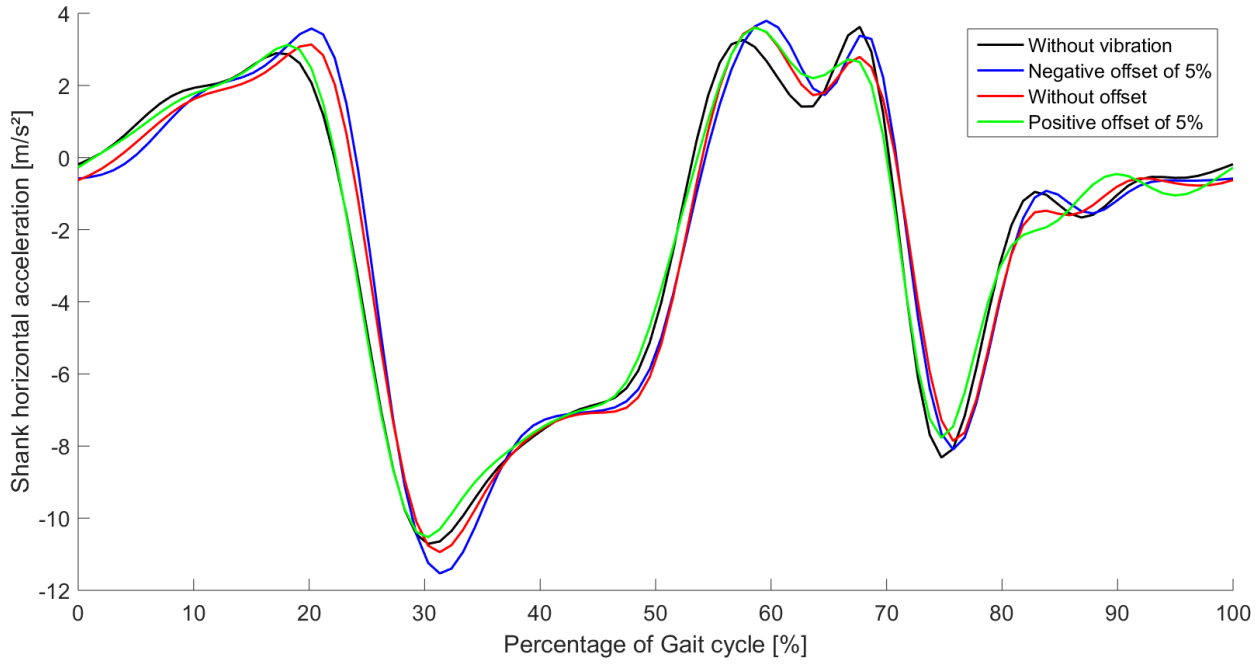

(b)

Figure 27: *Graph of the shank horizontal acceleration [m/s^2] for (a) the stimulated leg and (b) the non-stimulated leg, with the condition where there is no stimulation applied in black, where the stimulation is applied with a negative offset of 5% in blue, where it is applied without any offset in red and with a positive offset of 5% in green.*

2.2. Time offset between each condition

The point chosen for this analysis is the second maximum occurring after the stimulation, encircled in red in Figure 27a. The first maximum cannot be chosen because it does not appear in the signal of some of the subjects. A one-way repeated measures ANOVA on this variable gives a p-value of 0.235 (GG) for the right leg and of 0.674 (GG) for the left leg. Therefore, the null hypothesis cannot be rejected. The means of this variable for each condition for both legs are given in Figure 29.

3. Shank vertical acceleration

3.1. Amplitude

In Figure 30, it can be observed that the main difference between signals occurs between the peak-to-peak amplitudes. The two-way repeated measures ANOVA for this variable gives a p-value of 0.256 (GG) for the effects of conditions only, 0.904 for the effects of legs only and 0.0005 (GG) for the effects of the interaction of those factors. Therefore, only the interaction of both factors has an effect on the peak-to-peak amplitudes. The differences in the means between conditions for both legs are shown in Figure 31.

To determine for which pair of conditions and for which leg the means are significantly different, a pairwise t-test is completed (Table B3 in Appendix B on page 75). The only p-value below the significant level $\alpha = 0.05$ is the one of the pair of conditions where there is no stimulation applied compared to the one where the stimulation is applied without any offset for the right leg (0.04). It appears that the peak-to-peak amplitude of the first condition (mean of 15.6 m/s^2) is higher than the one of the second condition (mean of 14.4 m/s^2), which can be observed in Figure 32.

3.2. Time offset between each condition

The point chosen for this analysis is the global maximum, which occurs after the stimulation. A one-way repeated measures ANOVA on this variable gives a p-value of 0.356 (GG) for the right leg and of 0.084 (HF) for the left leg. Therefore, the null hypothesis cannot be rejected, so there is no difference in means of the occurrence time of the maximum between the conditions for both legs. The means of this variable for each condition and each leg are given in Figure 33.

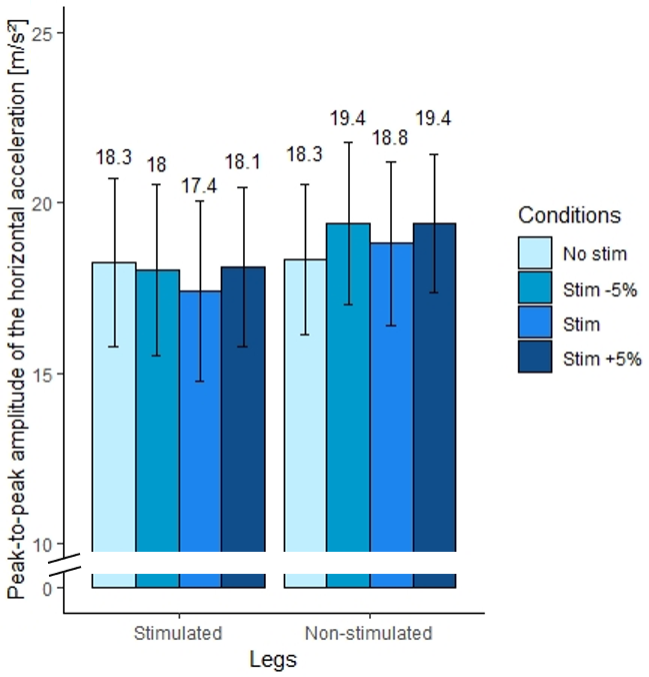

Figure 28: *Comparison of the peak-to-peak amplitudes of the shank horizontal acceleration [m/s^2] for each leg and each condition. The means are represented by the bars and the standard deviations by the vertical lines.*

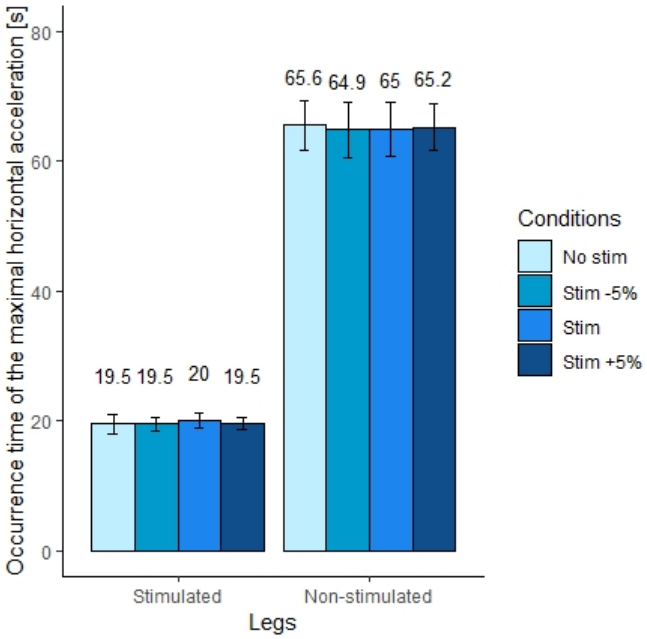

Figure 29: *Comparison of the occurrence times [s] of the second maximum of the shank horizontal acceleration just after the stimulation. The means are represented by the bars and the standard deviations by the vertical lines.*

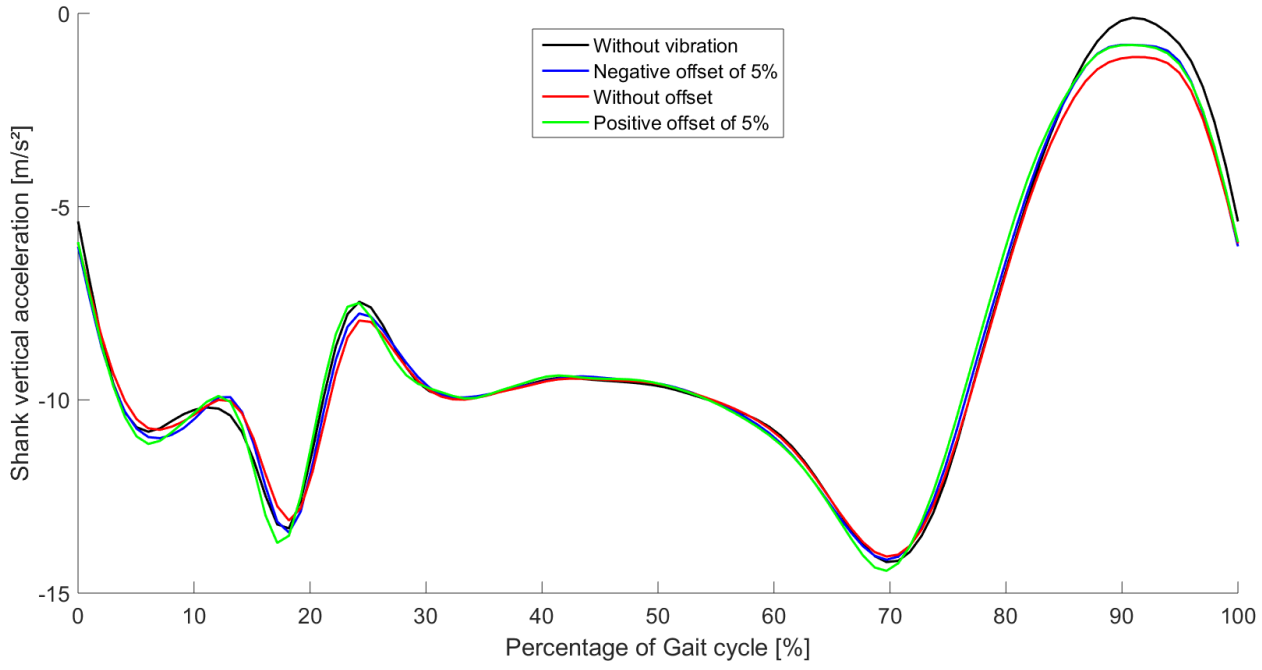

(a)

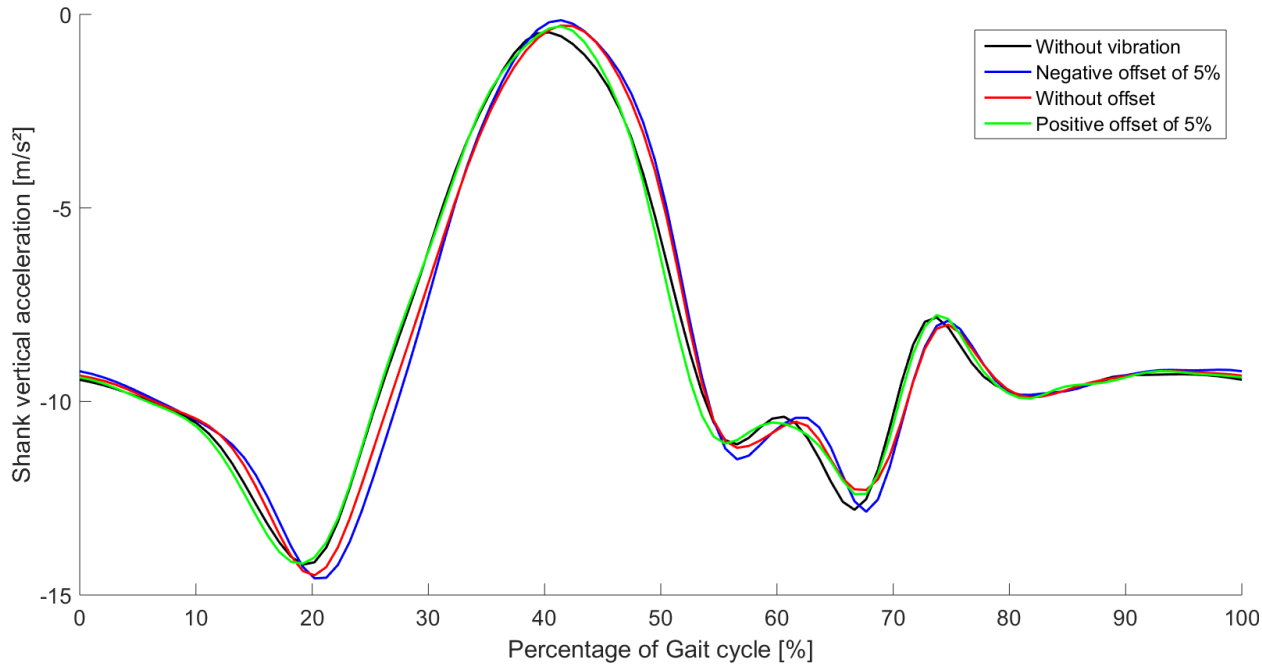

(b)

Figure 30: *Graph of the shank vertical acceleration [m/s^2] for (a) the stimulated leg and (b) the non-stimulated leg, with the condition where there is no stimulation applied in black, where the stimulation is applied with a negative offset of 5% in blue, where it is applied without any offset in red and with a positive offset of 5% in green.*

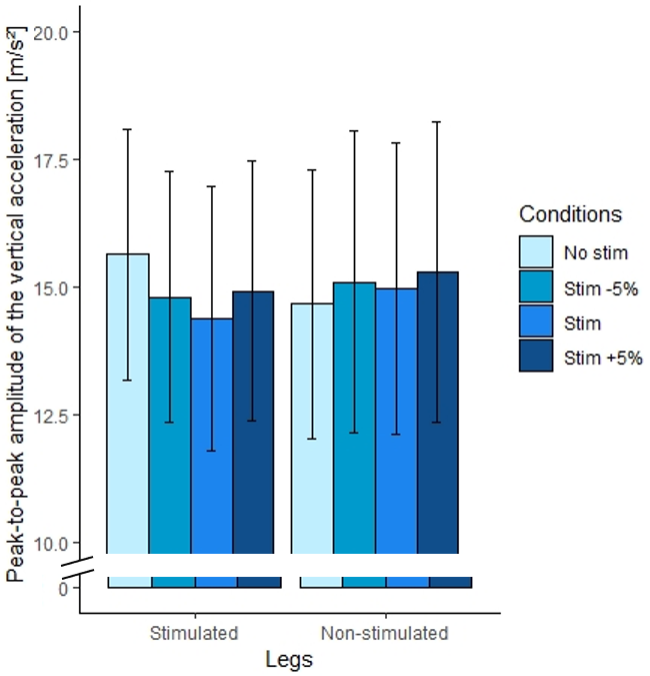

Figure 31: *Comparison of the peak-to-peak amplitudes of the shank vertical acceleration [m/s^2] for each leg and each condition. The means are represented by the bars and the standard deviations by the vertical lines.*

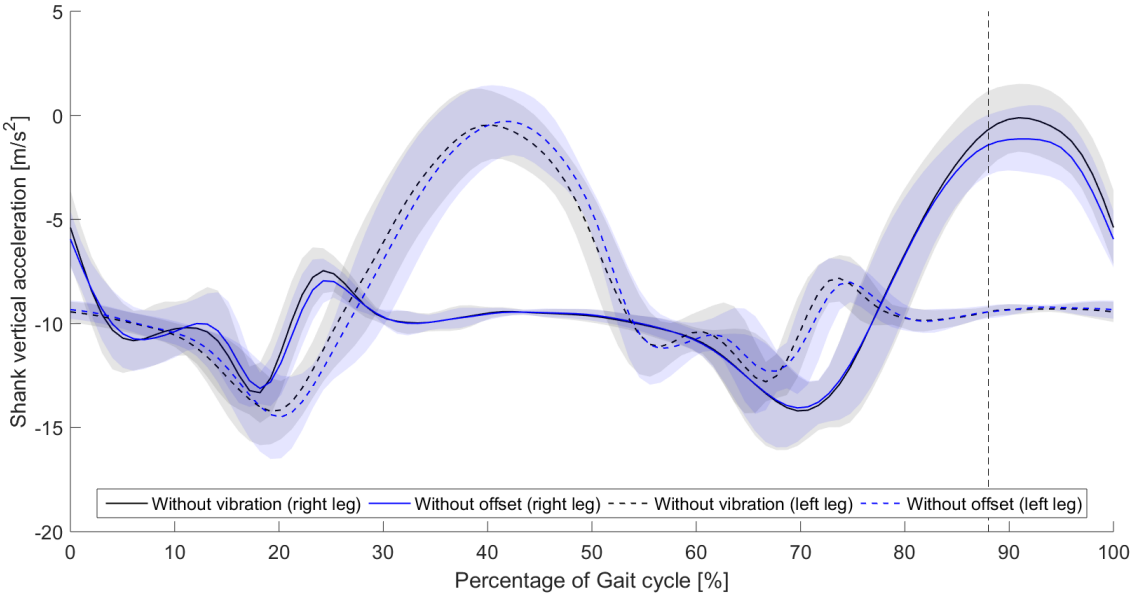

Figure 32: *Graph of the shank vertical acceleration of the stimulated leg (solid line) and of the non-stimulated leg (dashed line) for the pair of conditions where there is no stimulation applied (black) and where the stimulation is applied at the maximum knee flexion (blue). The shaded area represents the standard deviation for each signal and the vertical dashed line the maximum knee flexion.*

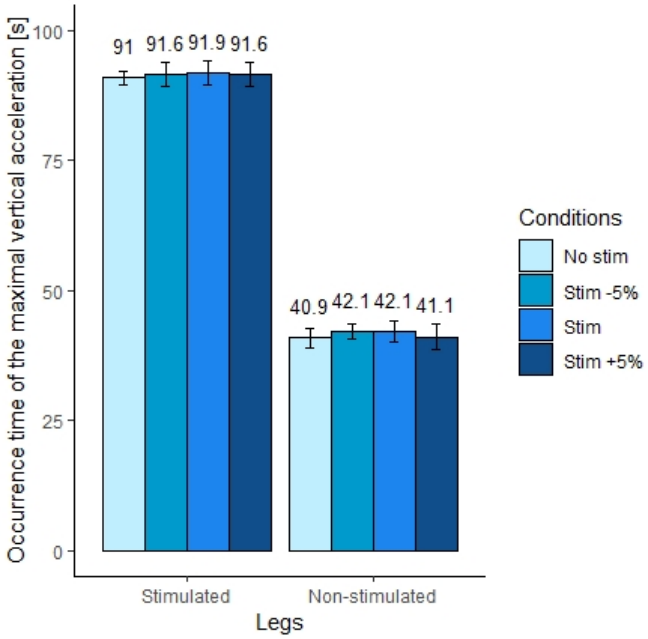

Figure 33: *Comparison of the occurrence times [s] of the maximum of the shank vertical acceleration. The means are represented by the bars and the standard deviations by the vertical lines.*

4. Summary

The main results concern two categories of parameters. For the first one, the temporal parameters, the results are:

- No difference in stride durations between legs and stimulation conditions;
- No change in phase leads between the legs for all the conditions;
- No time offset of the signals between conditions.

For the second one, the spatial parameters, the results are:

- The maximum amplitude of the shank angular velocity is higher in the condition where there is no vibration applied than in the one where the stimulation is applied at the maximum knee flexion;
- The peak-to-peak amplitude of the shank vertical acceleration is higher in the condition where there is no vibration applied than in the one where the stimulation is applied at the maximum knee flexion.

The following chapter will interpret these results.

Chapter 5

Discussion

In this chapter, all the results presented in the previous chapter are discussed. The effects of the experimental conditions on the temporal parameters are firstly analysed, followed by their effects on spatial parameters. We will finish by explaining the limits of this study and by giving some perspectives for future works.

1. Effects on temporal parameters

The previous chapter showed that there is no effect of the different experimental conditions on the temporal aspects of the signals. Firstly, there is no change in the phase lead between both legs. This agrees with the results of Verschueren and colleagues [42]. They found that the phase between the legs was not perturbed by the vibration, except when the biceps femoris was stimulated, which is not the case in this work. Secondly, the stride durations stay the same between all conditions, which is consistent with the fact that there is no offset between occurrence times of particular events in the signals.

Therefore, the stimulation does not act on the temporal parameters between experimental conditions or between legs. This agrees with our hypothesis that these parameters should not change for the condition where the stimulation is applied at the maximum knee flexion, but not with our hypotheses that they should change for the two conditions where the stimulation is applied with an offset (see Section 2 of Chapter 3 on page 35). However, to the best of our knowledge, no article studied the effects of an offset introduced in the delivering time of a vibrotactile stimulation applied on a tendon, and therefore no article proved that this perturbation should influence the temporal parameters of the gait cycle. We can conclude that our hypotheses for these two last conditions were probably wrong.

2. Effects on spatial parameters

On the one hand, the absence of effects on the amplitudes of the signals of the non-stimulated leg is consistent with the results of Verschueren and colleagues [42]. Indeed, their conclusion was that "the proprioceptive information of one limb does not appear to influence joint displacement in the other limb".

On the other hand, the only effect observed on the stimulated leg was between the condition where there is no stimulation applied and where the vibration was applied at the maximum knee flexion. The effects appear on two signals: the shank angular velocity and the shank vertical acceleration. For both signals, the amplitude was higher for the first condition than for the second. Indeed, due to the vibration, the tendon feels like it is more lengthened that it really is. Therefore, the subject does not conclude his movement: the rotation movement of the shank at the mid swing phase, just after the stimulation, is slower and he also slows down the upward movement of the shank that follows the maximum knee flexion (Figure 34). This agrees with our hypothesis that the stimulation should have an effect on spatial parameters when it is applied at the maximum knee flexion (see Section 2 of Chapter 3 on page 35). This also agrees with the conclusion of Mildren and Bent [45] that vibrotactile stimulations can impair proprioceptive information of the joint.

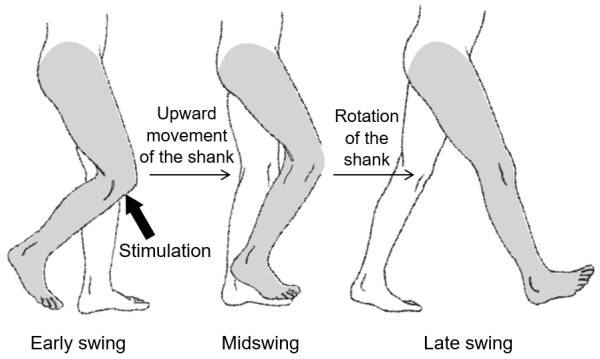

Figure 34: *Movements of the shank at mid swing, adapted from [83].*

In contrast, it is surprising to observe no effect of the other experimental conditions, especially after having obtained results for the condition where the stimulation is applied without any offset. Indeed, we expected to observe that the movement will be shortened in the condition where the stimulation is applied 5% before the maximum knee flexion, and that the movement will be extended in the condition where the stimulation is applied 5% after this event (see Section 2 of Chapter 3 on page 35). One could think that this is due to the fact that the value of 5% is too small and therefore that the CNS does not feel the offset in the delivering time of the stimulation. However, if this was the case, these conditions should give the same results as the condition where the stimulation is applied without any offset,

which is not the case. To be able to explain this phenomenon, some additional experiments and analysis have to be performed. Based on this work, no conclusion can be drawn.

Finally, it was interesting to notice that only two among the eight subjects actually felt the stimulation. This shows that the stimulation was really unconscious and that subjects integrated the discrete stimulation in their walking scheme, as suggested by Crea and colleagues [36]. Moreover, by comparing the results of the two subjects that felt the vibration to the others, there was no difference. Their gait parameters were also perturbed. Therefore, it proves that a vibrotactile stimulation, whether perceived or not, can perturb the spatial parameters of the gait cycle of able-bodied subjects.

3. Limits of this study

A major drawback of this work is that the gait phase signal used to activate the vibration is not accurate. Indeed, this signal does not always reset to 0 exactly at the gait event detection, but sometimes with a little delay. Therefore, we cannot be completely sure that the vibration is activated at the maximum knee flexion. In this work, it is only an assumption, but for subsequent works it has to be a certainty. To solve this problem, cameras from the NMSK lab of UCLouvain can be synchronized with the gait signal, and a third IMU fixed on a second vibrotactile unit can be used to detect the times where the vibration is activated. In that way, we can verify that the stimulation arises at the desired time.

The most challenging part of this work is to accurately detect a gait event in order to apply the vibration at the desired time. For this, the heel strike has to be correctly detected. In this work, our algorithm using shank angular velocity failed to detect it and we had to use the mid swing peak as the beginning of a gait cycle. A different approach might provide better results. Moreover, a more robust method has to be used, because gyroscope signals are great for gait cycle segmentation in gait of able-bodied subjects, but maybe not for the gait of amputees.

A first solution is to use the acceleration signals from the IMUs, instead of the angular velocity signals. In the study of Khandelwal and Wickström [84], three-axes accelerometers were attached to both ankles. To avoid misalignment issues, the composite acceleration signal is used, which corresponds to the squared root of the sum of squared accelerations in the three directions. The heel strike corresponds to the peaks in the signal (Figure 35).

An alternative solution is to use sensorized insoles instead of IMUs. In general, the sum of all the FRS sensors, called "sumFRS", contained in the insole is used to detect the heel strike and toe off phases. It has the advantage of not being noisy, and therefore no preprocessing or

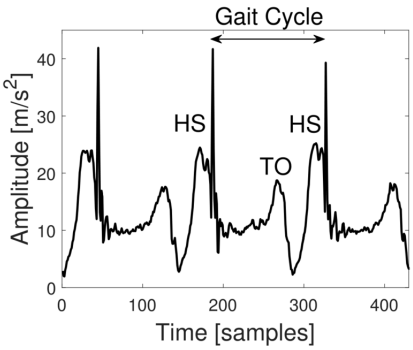

Figure 35: *Composite acceleration signal calculated based on IMUs signals to detect heel strikes [84].*

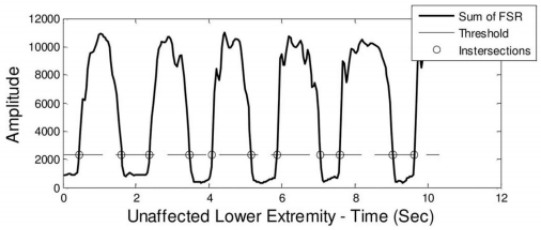

Figure 36: *Signal of the sum of the FRS sensors contained into the sensorized insole [85].*

denoising algorithms have to be performed. In the method proposed by Lopez-Meyer, Fulk and Sazonov [85], a detection threshold is computed by using the average of maxima and of minima in the sumFRS signal. The intersections of this threshold with the sumFRS signal correspond to heel strike and toe off points. Heel strike corresponds to the intersection just after a local minima (Figure 36).

Other limits of this work concern the filtering of the signals. The filter used (see Section 5.2 of Chapter 3 on page 47) induces a delay. Therefore, to be more accurate, we should have use a zero-phase filter by processing the signal in the forward and then backward directions [86]. In that case, the filter does not induce any delay.
Moreover, the order of the Butterworth filter was maybe too strong and therefore attenuated some of the fluctuations in the signals (Figure 21 on page 48). Hence, some results are maybe also attenuated or even not observed.

4. Perspectives

The results of this work may potentially be used for rehabilitation of lower-limb amputees by adaptation to a perturbation. Indeed, if the shank angular velocity of the amputated limb has a lower amplitude at the mid swing phase than the one of the sound limb, as shown in Figure 37 for a transfemoral amputee, a vibration can be applied on the sound limb to decrease the angular velocity amplitude at mid swing. Therefore, the gait symmetry would be restored. However, this potential effect has to be confirmed by analysing gait patterns of transtibial amputees. Moreover, it has to be observed if the effect of the stimulation stays in time, even when the stimulation is not applied anymore. Nevertheless, even if it is not the case, a device could be developed to apply the stimulation in everyday life.

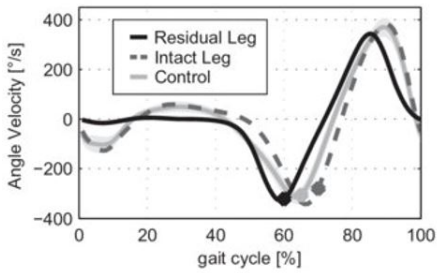

Figure 37: *Knee angular velocity of the amputated limb (black) compared to the intact limb (dashed grey line) of a transfemoral amputee [87].*

For purposes of developing a prosthesis providing artificial sensory feedback to the user, it would be interesting to deepen what was previously done in the literature. Indeed, most of the studies using a vibrotactile stimulus applied a stimulation concurrently with a gait event on the lower back or on the thigh of the patient. These studies raised some questions to improve knowledge about artificial feedback provided to lower-limb amputees:

- Which location between the lower back and the thigh is the most sensitive to vibrotactile stimulation? Is there any differences in performances of lower-limb amputees between a stimulation applied at the lower back or at the thigh?
- Is there any differences in performance of lower-limb amputees between a discrete stimulation and a stimulation using the tactile phi phenomenon? (See Section 1.2 in Chapter 2 on page 14).
- How to develop a robust gait event detection algorithm for specific lower-limb amputees gait patterns?

As far as we know, the two first points have not yet been analysed, but some researches have studied the third point.

Conclusion

Adding an artificial sensory feedback to lower-limb prostheses is one of the challenges left in this domain. Indeed, the lack of this feedback, in addition to the loss of motor functions, leads to abnormal gait kinematics, which cause a lot of additional medical conditions and induce a high rejection rate of the prosthesis by patients. This thesis is part of the research on sensory feedback for lower-limb amputees. Its goal was to analyse the effects of tendon vibration on gait pattern of able-bodied subjects. If it influences their gait cycle, it could be adapted and used in transtibial amputees.

The literature review showed that nowadays the main way to provide an artificial sensory feedback is to transmit to the subject information about a gait parameter thanks to a stimulus applied on the thigh or on the lower back. We also saw that muscle tendon vibration can induce an illusory movement, which is one of the results that was used for this work. Finally, we saw that adaptation to a perturbation is a form of motor learning that can be used in order for the lower-limb amputee to acquire new motor skills and strategies.

The chapter about the materials and methods explained how the experiments were conducted. The site where the stimulation was applied was the right patellar tendon of the knee. Since tendon vibration had been shown to induce a lengthening illusion of the muscle connected to it, the vibration was applied at the maximum knee flexion, when the quadriceps muscle and the patellar tendon are maximally stretched.
The experiments used four different conditions: (1) no stimulation is applied, (2) the vibration is applied at the maximum knee flexion, (3) 5% of the gait cycle before this event and (4) 5% of the gait cycle after this event. In order to apply these stimulations at the desired time, inertial measurement units were fixed on the side of each shank. The right angular velocity around the z-axis provided by these devices was learned by adaptive oscillators. This allowed to obtain a smoother signal without adding a delay due to filtering. Therefore, the signal given by the adaptive oscillators allowed to identify a particular gait event in real-time. This event was chosen to be the mid swing phase, corresponding to a global maximum in the angular velocity signal of one gait cycle. Therefore, the stimulation had to be applied at 88% of the gait cycle starting from this event, which corresponds to the moment where the knee is maximally flexed. In order to determine at which percent of the gait cycle we are in real-time,

the gait phase signal was used. This signal goes from 0 to 100% between two detected events.

The results of the eight able-bodied subjects showed that there was no effect of the stimulation on temporal parameters. Indeed, the phase lead between the legs was not perturbed, as well as the stride durations between the experimental conditions. In contrast, effects were observed on the amplitudes of the shank angular velocity and of the vertical acceleration signals. Indeed, the amplitudes of the signals for the condition where there is no stimulation applied were higher than those for the condition where the stimulation is applied at the maximum knee flexion. This is due to the lengthening illusion induced by muscle tendon vibration, that causes the subject to not conclude his movement. Surprisingly, no effect was found between these conditions and the two where the stimulation is applied with an offset with respect to the maximum knee flexion.

To conclude the discussion, some perspectives of this work were given. Firstly, the perturbation induced by the tendon vibration can potentially be used as a rehabilitation therapy for lower-limb amputees. Indeed, it could help to restore the gait symmetry between the amputated and sound limbs. However, this is only an assumption which has to be confirmed by analysis of gait patterns of lower-limb amputees.
For next steps in research on sensory feedback for lower-limb amputees, it was suggested to explore three different aspects of the stimulation, in order to deepen the knowledge in this field. Firstly, the differences in performances between a stimulation applied at the lower back or at the thigh should be studied. Secondly, the differences in performances between a discrete stimulation and a stimulation using the tactile phi phenomenon should also be analysed. Finally, a robust gait event detection algorithm for lower-limb amputees should be developed. This last point was unfortunately the weak point of this work.

In conclusion, a vibration applied at the patellar tendon of the knee effectively induced a perturbation of some spatial parameters. However, it does not perturb temporal parameters. Therefore, it proves that a vibrotactile stimulation applied at the patellar tendon influences the gait pattern of able-bodied subjects.

Appendices

A. Repeated measures ANOVA assumptions

The different assumptions of the repeated measures ANOVA are the following [80].

A.1. Continuity of the dependent variable

All the dependent variables chosen for the statistical analysis are continuous: the stride duration [s], the phase lead [%], the amplitude of the angular velocity [°/s] or of the acceleration [m/s^2] and the apparition time of the maximum just after the stimulation [s].

A.2. Sphericity

Sphericity indicates that the variances of the differences between all combinations of conditions are equal [88]. When this condition is violated, the Greenhouse-Geisser correction and the Huynd-Feldt correction can be applied. They both estimate the degree of sphericity $\hat{\varepsilon}$ [88]. If $\hat{\varepsilon} < 0.75$ for both corrections, the GG correction is used. If $\hat{\varepsilon} > 0.75$ for both corrections, the HF correction is chosen [79].

A.3. Normality of the distribution of the dependent variable

The Shapiro-Wilk test is used, as it is powerful for relatively small sample sizes [89]. It is based on the W statistic. The condition to reject the normality is $W < W_{crit}$, with W_{crit} given in the Shapiro-Wilk table [90].

If we consider $\alpha = 0.05$, the critical value for $n = 8$ subjects is $W_{crit} = 0.818$. The results of this normality test are given in Tables A1 to A7. The data that are not normally distributed are highlighted in red in the following tables. This concerns the data for stride durations and phase leads in the condition where the stimulation is applied 5% before the maximum knee flexion and for the occurrence time of the maximum of the horizontal acceleration amplitude of the right leg for the stimulation without any offset.

Table A1: *Values of the W statistics for the stride durations.*

Conditions	Right leg	Left leg
No stimulation	0.884	0.884
Stimulation with an offset of -5%	0.810	0.810
Stimulation without offset	0.859	0.867
Stimulation with an offset of +5%	0.868	0.859

Table A2: *Values of the W statistics for the phase leads between legs.*

Conditions	
No stimulation	0.897
Stimulation with an offset of -5%	0.798
Stimulation without offset	0.848
Stimulation with an offset of +5%	0.883

Table A3: *Values of the W statistics for the maximum amplitudes of the shank angular velocity.*

Conditions	Right leg	Left leg
No stimulation	0.954	0.974
Stimulation without an offset of -5%	0.933	0.964
Stimulation without offset	0.955	0.952
Stimulation with an offset of -5%	0.941	0.979

Table A4: *Values of the W statistics for the peak-to-peak amplitudes of the shank horizontal acceleration.*

Conditions	Right leg	Left leg
No stimulation	0.908	0.947
Stimulation without an offset of -5%	0.919	0.947
Stimulation without offset	0.932	0.933
Stimulation with an offset of -5%	0.956	0.938

Table A5: *Values of the W statistics for the occurrence times of the maximum of the shank horizontal acceleration.*

Conditions	Right leg	Left leg
No stimulation	0.891	0.820
Stimulation without an offset of -5%	0.860	0.830
Stimulation without offset	0.815	0.873
Stimulation with an offset of -5%	0.931	0.891

Table A6: *Values of the W statistics for the peak-to-peak amplitudes of the shank vertical acceleration.*

Conditions	Right leg	Left leg
No stimulation	0.959	0.989
Stimulation with an offset of -5%	0.883	0.984
Stimulation without offset	0.938	0.971
Stimulation with an offset of +5%	0.962	0.982

Table A7: *Values of the W statistics for the occurrence times of the maximum of the shank vertical acceleration.*

Conditions	Right leg	Left leg
No stimulation	0.96507	0.792
Stimulation with an offset of -5%	0.971	0.930
Stimulation without offset	0.965	0.946
Stimulation with an offset of +5%	0.928	0.952

B. Results of the pairwise t-tests

The results of the pairwise t-tests for the repeated-measures ANOVAs that gave a p-value lower than $\alpha = 0.05$ are given in Tables B1 to B2. The effect size indicates to what extent the condition has an effect on the measured variable. It can be observed that the pairs of conditions having a p-value lower than 0.05 (highlighted in red) have also a greater effect size than the other pairs, which is logical. The other pairs have very small effect sizes, in particular the pairs of conditions with an offset.

Table B1: *P-values for the pairwise t-test on the maximum amplitudes of the shank angular velocity.*

Leg	Pair of conditions	p-value	Effect size
Right	No stimulation - Stimulation without offset	0.039	0.413
	No stimulation - Stimulation with an offset of -5%	0.985	0.130
	No stimulation - Stimulation with an offset of +5%	0.985	0.113
	Stimulation without offset - Stimulation with an offset of -5%	0.058	0.264
	Stimulation without offset - Stimulation with an offset of +5%	0.149	0.255
	Stimulation with an offset of -5% - Stimulation with an offset of +5%	1	0.008
Left	No stimulation - Stimulation without offset	0.120	0.248
	No stimulation - Stimulation with an offset of -5%	0.072	0.363
	No stimulation - Stimulation with an offset of +5%	0.119	0.373
	Stimulation without offset - Stimulation with an offset of -5%	0.277	0.114
	Stimulation without offset - Stimulation with an offset of +5%	0.828	0.135
	Stimulation with an offset of -5% - Stimulation with an offset of +5%	1	0.026

Table B2: *p-values for the pairwise t-test on the peak-to-peak amplitudes of the shank horizontal acceleration.*

Leg	Pair of conditions	p-value
Right	No stimulation - Stimulation without offset	0.691
	No stimulation - Stimulation with an offset of -5%	1
	No stimulation - Stimulation with an offset of +5%	1
	Stimulation without offset - Stimulation with an offset of -5%	0.089
	Stimulation without offset - Stimulation with an offset of +5%	0.329
	Stimulation with an offset of -5% - Stimulation with an offset of +5%	1
Left	No stimulation - Stimulation without offset	0.350
	No stimulation - Stimulation with an offset of -5%	0.220
	No stimulation - Stimulation with an offset of +5%	0.200
	Stimulation without offset - Stimulation with an offset of -5%	0.370
	Stimulation without offset - Stimulation with an offset of +5%	0.430
	Stimulation with an offset of -5% - Stimulation with an offset of +5%	1

Table B3: *p-values for the pairwise t-test on the peak-to-peak amplitudes of the shank vertical acceleration.*

Leg	Pair of conditions	p-value	Effect size
Right	No stimulation - Stimulation without offset	0.040	0.500
	No stimulation - Stimulation with an offset of -5%	0.670	0.338
	No stimulation - Stimulation with an offset of +5%	0.710	0.286
	Stimulation without offset - Stimulation with an offset of -5%	0.301	0.167
	Stimulation without offset - Stimulation with an offset of +5%	0.230	0.210
	Stimulation with an offset of -5% - Stimulation with an offset of +5%	1	0.047
Left	No stimulation - Stimulation without offset	1	0.110
	No stimulation - Stimulation with an offset of -5%	1	0.153
	No stimulation - Stimulation with an offset of +5%	0.530	0.228
	Stimulation without offset - Stimulation with an offset of -5%	1	0.043
	Stimulation without offset - Stimulation with an offset of +5%	0.540	0.115
	Stimulation with an offset of -5% - Stimulation with an offset of +5%	0.660	0.070

Bibliography

[1] S. Kishner and J. Laborde. Gait Analysis After Amputation. https://emedicine.medscape.com/article/1237638-overview#a2, 2018.

[2] K. Ziegler-Graham, E. MacKenzie, P. Ephraim, T. Travison, and R. Brookmeyer. Estimating the Prevalence of Limb Loss in the United States: 2005 to 2050. *Archives of Physical Medicine and Rehabilitation*, 89(3):422–429, 2008.

[3] I. de Thysebaert. *Augmented feedback for lower-limb amputees - Gait perturbation by vibrotactile stimulation of the patellar tendon: proof of concept.* Master thesis, Université Catholique de Louvain, 2018.

[4] Nova Scotia Health Authority. Lower Limb Amputations. http://www.cdha.nshealth.ca/amputee-rehabilitation-musculoskeletal-program/patient-family-information/lower-limb-amputations.

[5] E. Mastinu, P. Doguet, Y. Botquin, B. Hakansson, and M. Ortiz-Catalan. Embedded System for Prosthetic Control Using Implanted Neuromuscular Interfaces Accessed Via an Osseointegrated Implant. *IEEE Transactions on Biomedical Circuits and Systems*, 11(4):867–877, 2017.

[6] N. Fallahian, H. Saeedi, H. Mokhtarinia, and F. Tabatabai Ghomshe. Sensory feedback add-on for upper-limb prostheses. *Prosthetics and Orthotics International*, 41(3):314–317, 2017.

[7] European Commission. Artificial limbs allowing amputees to touch and sense again. https://ec.europa.eu/digital-single-market/en/news/artificial-limbs-allowing-amputees-touch-and-sense-again,
2017.

[8] A. Sharma, R. Torres-Moreno, K. Zabjek, and J. Andrysek. Toward an artificial sensory feedback system for prosthetic mobility rehabilitation: Examination of sensorimotor responses. *Journal of Rehabilitation Research and Development*, 51(6):907–917, 2014.

[9] S. Crea, C. Cipriani, M. Donati, M. C. Carrozza, and N. Vitiello. Providing time-discrete gait information by wearable feedback apparatus for lower-limb amputees: usability and functional validation. *IEEE Transactions on Neural Systems and Rehabilitation Engineering*, 23(2):250–7, 2015.

[10] R. Gailey. Review of secondary physical conditions associated with lower-limb amputation and long-term prosthesis use. *Journal of Rehabilitation Research and Development*, 45(1):15–29, 2008.

[11] D. Purves, G. Augustine, D. Fitzpatrick, W. Hall, A.-S. LaMantia, R. Mooney, M. Platt, and L. White. The Somatosensory System: Touch and Proprioception. In *Neurosciences*, chapter Unit II: S, pages 193–211. Oxford University Press, New-York, 6th edition, 2018.

[12] P. Houglum and D. Bertoti. Chapter 3: The Movement System: Nerve and Muscle Physiology and the Control of Human Movement. In *Brunnstrom's Clinical Kinesiology*. 2012.

[13] J. Duqué. Le système somesthésique. In *LIEPR1024 - Fondements neurophysiologiques et neuropsychologiques du contrôle et de l'apprentissage moteurs*, pages 6–12. Université Catholique de Louvain, 2018.

[14] T. Kernozek and J. Willson. Gait. https://clinicalgate.com/gait-2/, 2015.

[15] M. Tucker, J. Olivier, A. Pagel, H. Bleuler, M. Bouri, O. Lambercy, J. d. R. Millán, R. Riener, H. Vallery, and R. Gassert. Control strategies for active lower extremity prosthetics and orthotics: a review. *Journal of Neuroengineering and Rehabilitation*, 12(1):1–29, 2015.

[16] J. B. Nielsen and T. Sinkjaer. Afferent feedback in the control of human gait. *Journal of Electromyography and Kinesiology*, 12(3):213–217, 2002.

[17] B. Stephens-Fripp, G. Alici, and R. Mutlu. A Review of Non-Invasive Sensory Feedback Methods for Transradial Prosthetic Hands. *IEEE Access*, 6:6878–6899, 2018.

[18] C. Günter, J. Delbeke, and M. Ortiz-Catalan. Safety of long-term electrical peripheral nerve stimulation: review of the state of the art. *Journal of NeuroEngineering and Rehabilitation*, 16(1):13, 2019.

[19] K. Collins, A. Guterstam, J. Cronin, J. Olson, H. Ehrsson, and J. Ojemann. Ownership of an artificial limb induced by electrical brain stimulation. *Proceedings of the National Academy of Sciences*, 114(1):166–171, 2017.

[20] IGI Global. What is Electrocutaneous (or electrotactile) Stimulation. https://www.igi-global.com/dictionary/electrocutaneous-stimulation-skin-mechanoreceptors-tactile/9267.

[21] M. D'Alonzo, S. Dosen, C. Cipriani, and D. Farina. HyVE: hybrid vibro-electrotactile stimulation for sensory feedback and substitution in rehabilitation. *IEEE Transactions on Neural Systems and Rehabilitation Engineering*, 22(2):290–301, 2014.

[22] A. Pagel, A. H. Arieta, R. Riener, and H. Vallery. Effects of sensory augmentation on postural control and gait symmetry of transfemoral amputees: a case description. *Medical & Biological Engineering & Computing*, 54(10):1579–1589, 2016.

[23] D. Buma, J. Buitenweg, and P. Veltink. Intermittent Stimulation Delays Adaptation to Electrocutaneous Sensory Feedback. *IEEE Transactions on Neural Systems and Rehabilitation Engineering*, 15(3):435–441, 2007.

[24] J. Sabolich and G. Ortega. Sense of Feel for Lower-Limb Amputees: A Phase-One Study. *Journal of Prosthetics and Orthotics*, 6(2), 1994.

[25] J. Sabolich, G. Ortega, and B. Schwabe. Patent US6500210B1: System and method for providing a sense of feel in a prosthetic or sensory impaired limb, 1996.

[26] Scott Sabolich Prosthetics & Research. Research & Development. http://www.scottsabolich.com/research-development/.

[27] K. Kaczmarek. Electrotactile adaptation on the abdomen: preliminary results. *IEEE Transactions on Rehabilitation Engineering*, 8(4):499–505, 2000.

[28] G. Webb, S. Ghoussayni, and D. Ewins. Electrotactile feedback for trans-femoral amputee gait re-education. In *First Annual Conference of the UKRI-IFESS*, 2010.

[29] G. Webb. Providing Real-time Biofeedback for Amputee Gait re-training. In *NIDays Worldwide Graphical System Design Conference*, pages 54–55, 2009.

[30] S. Pfeifer, O. Çaldıran, H. Vallery, and A. Hernandez Arieta. Displaying centre of pressure location by electrotactile stimulation using phantom sensation. In *10th Vienna International Workshop on Functional Electrical Stimulation and 15th IFESS Annual Conference*, Vienna, 2010.

[31] G. Webb, S. Cirovic, S. Ghoussayni, and D. Ewins. Electro-tactile sensation thresholds for an amputee gait-retraining system. In *3rd Annual Conference of the International Functional Electrical Stimulation Society*, 2012.

[32] D. Zambarbieri, M. Schmid, and V. Gennaro. Sensory feedback for lower limb prostheses. In *Intelligent systems and technologies in rehabilitation engineering*, pages 129–151. 2001.

[33] E. Wentink, A. Mulder, J. Rietman, and P. Veltink. Vibrotactile stimulation of the upper leg: Effects of location, stimulation method and habituation. In *2011 Annual International Conference of the IEEE Engineering in Medicine and Biology Society*, volume 2011, pages 1668–1671. IEEE, 2011.

[34] D. Rusaw, K. Hagberg, L. Nolan, and N. Ramstrand. Can vibratory feedback be used to improve postural stability in persons with transtibial limb loss? *Journal of rehabilitation research and development*, 49(8):1239–1254, 2012.

[35] A. Sharma, M. Leineweber, and J. Andrysek. Effects of cognitive load and prosthetic liner on volitional response times to vibrotactile feedback. *Journal of Rehabilitation Research and Development*, 53(4):473–482, 2016.

[36] S. Crea, B. Edin, K. Knaepen, R. Meeusen, and N. Vitiello. Time-Discrete Vibrotactile Feedback Contributes to Improved Gait Symmetry in Patients With Lower Limb Amputations: Case Series. *Physical Therapy*, 97(2):198–207, 2017.

[37] A. Wan, D. Wong, C. Ma, M. Zhang, and W. Lee. Wearable Vibrotactile Biofeedback Device Allowing Identification of Different Floor Conditions for Lower-Limb Amputees. *Archives of Physical Medicine and Rehabilitation*, 97(7):1210–1213, 2016.

[38] A. Plauche, D. Villarreal, and R. Gregg. A Haptic Feedback System for Phase-Based Sensory Restoration in Above-Knee Prosthetic Leg Users. *IEEE Transactions on Haptics*, 9(3):421–426, 2016.

[39] B. Chen, Y. Feng, and Q. Wang. Combining vibrotactile feedback with volitional myoeletric control for robotic transtibial prostheses. *Frontiers in Neurorobotics*, 10:Article number: 8, 2016.

[40] C. Lauretti, G. Pinzari, A. L. Ciancio, A. Davalli, R. Sacchetti, S. Sterzi, E. Guglielmelli, and L. Zollo. A vibrotactile stimulation system for improving postural control and knee joint proprioception in lower-limb amputees. In *2017 26th IEEE International Symposium on Robot and Human Interactive Communication (RO-MAN)*, pages 88–93. IEEE, 2017.

[41] M. D'Alonzo, S. Dosen, C. Cipriani, and D. Farina. HyVE—Hybrid Vibro-Electrotactile Stimulation—Is an Efficient Approach to Multi-Channel Sensory Feedback. *IEEE Transactions on Haptics*, 7(2):181–190, 2014.

[42] S. Verschueren, S. Swinnen, K. Desloovere, and J. Duysens. Effects of tendon vibration on the spatiotemporal characteristics of human locomotion. *Experimental Brain Research*, 143(2):231–239, 2002.

[43] F. Albert, M. Bergenheim, E. Ribot-Ciscar, and J.-P. Roll. The Ia afferent feedback of a given movement evokes the illusion of the same movement when returned to the subject via muscle tendon vibration. *Experimental Brain Research*, 172(2):163–174, 2006.

[44] J.-P. Roll, F. Albert, C. Thyrion, E. Ribot-Ciscar, M. Bergenheim, and B. Mattei. Inducing Any Virtual Two-Dimensional Movement in Humans by Applying Muscle Tendon Vibration. *Journal of Neurophysiology*, 101(2):816–823, 2009.

[45] R. Mildren and L. Bent. Vibrotactile stimulation of fast-adapting cutaneous afferents from the foot modulates proprioception at the ankle joint. *Journal of Applied Physiology*, 120(8):855–864, 2016.

[46] C. Sacco, E. Gaffney, and J. Dean. Effects of White Noise Achilles Tendon Vibration on Quiet Standing and Active Postural Positioning. *Journal of Applied Biomechanics*, 34(2):151–158, 2018.

[47] S. Gandevia. Illusory movements produced by electrical stimulation of low-threshold muscle afferents from the hand. *Brain : a journal of neurology*, 108:965–81, 1985.

[48] H. Kajimoto. Illusion of motion induced by tendon electrical stimulation. In *2013 World Haptics Conference (WHC)*, pages 555–558. IEEE, 2013.

[49] Y. Vandermeeren. Apprentissage procédural et plasticité. In *Kine1036 - Compléments de neurophysiologie*, pages 17–37. UCLouvain, 2018.

[50] A. Bubic, Y. Von Cramon, and R. Schubotz. Prediction, cognition and the brain. *Frontiers in Human Neuroscience*, 4:25, 2010.

[51] V. Della-Maggiore, S. Landi, and J. Villalta. Sensorimotor Adaptation. *The Neuroscientist*, 21(2):109–125, 2015.

[52] R. Shadmehr and T. Brashers-Krug. Functional stages in the formation of human long-term motor memory. *The Journal of neuroscience : the official journal of the Society for Neuroscience*, 17(1):409–19, 1997.

[53] T. Martin, J. Keating, H. Goodkin, A. Bastian, and W. Thach. Throwing while looking through prisms. II. Specificity and storage of multiple gaze-throw calibrations. *Brain : a journal of neurology*, 119:1199–211, 1996.

[54] D. Reisman, H. McLean, J. Keller, K. Danks, and A. Bastian. Repeated Split-Belt Treadmill Training Improves Poststroke Step Length Asymmetry. *Neurorehabilitation and Neural Repair*, 27(5):460–468, 2013.

[55] D. Reisman, R. Wityk, K. Silver, and A. Bastian. Locomotor adaptation on a split-belt treadmill can improve walking symmetry post-stroke. *Brain*, 130(7):1861–1872, 2007.

[56] D. Reisman, R. Wityk, K. Silver, and A. Bastian. Split-Belt Treadmill Adaptation Transfers to Overground Walking in Persons Poststroke. *Neurorehabilitation and Neural Repair*, 23(7):735–744, 2009.

[57] R. Roemmich, J. Nocera, E. Stegemöller, A. Hassan, M. Okun, and C. Hass. Locomotor adaptation and locomotor adaptive learning in Parkinson's disease and normal aging. *Clinical Neurophysiology*, 125(2):313–319, 2014.

[58] D. Martelli, L. Luo, J. Kang, U. J. Kang, S. Fahn, and S. Agrawal. Adaptation of Stability during Perturbed Walking in Parkinson's Disease. *Scientific Reports*, 7(1):17875, 2017.

[59] A. Houldin, K. Luttin, and T. Lam. Locomotor adaptations and aftereffects to resistance during walking in individuals with spinal cord injury. *Journal of Neurophysiology*, 106(1):247–258, 2011.

[60] K. Kaufman, M. Wyatt, P. Sessoms, and M. Grabiner. Task-specific fall prevention training is effective for warfighters with transtibial amputations. *Clinical orthopaedics and related research*, 472(10):3076–3084, 2014.

[61] R. Sheehan, C. Rábago, J. Rylander, J. Dingwell, and J. Wilken. Use of Perturbation-Based Gait Training in a Virtual Environment to Address Mediolateral Instability in an Individual With Unilateral Transfemoral Amputation. *Physical therapy*, 96(12):1896–1904, 2016.

[62] O. Kannape and H. Herr. Split-belt adaptation and gait symmetry in transtibial amputees walking with a hybrid EMG controlled ankle-foot prosthesis. In *2016 38th Annual International Conference of the IEEE Engineering in Medicine and Biology Society (EMBC)*, volume 2016, pages 5469–5472. IEEE, 2016.

[63] S. H. Kim, K. Reed, J. Kahle, and J. Highsmith. Gait symmetry in transfemoral amputees. In *American Academy of Orthotists & Prosthetists, 43rd Academy Annual Meeting & Scientific Symposium*, 2017.

[64] B. Contreras. Quad Tendon. https://bretcontreras.com/random-thoughts-55/quad-tendon/, 2019.

[65] R. Wilkerson and S. Fischer. Patellar Tendon Tear. https://orthoinfo.aaos.org/en/diseases–conditions/patellar-tendon-tear/, 2016.

[66] H. Çabuk and F. K. Çabuk. Mechanoreceptors of the ligaments and tendons around the knee. *Clinical Anatomy*, 29(6):789–795, 2016.

[67] Aphysionado. 2. Récepteurs somatosensoriels tendino-musculaires. https://sites.google.com/site/aphysionado/home/fonctionssn/somesthesie/rcptrsensoriel.

[68] R. N. Kirkwood, H. Gomes, R. F. Sampaio, E. Culham, and P. Costigan. Biomechanical analysis of hip and knee joints during gait in elderly subjects. *Acta Ortopédica Brasileira*, 15(5):267–271, 2007.

[69] x-io Technologies. Open source IMU and AHRS algorithms. http://x-io.co.uk/open-source-imu-and-ahrs-algorithms/, 2012.

[70] x-io Technologies. x-IMU. http://x-io.co.uk/x-imu/.

[71] Tactile Labs. Haptuator Planar. http://tactilelabs.com/products/haptics/haptuator-planar/.

[72] H.-Y. Yao and V. Hayward. Design and analysis of a recoil-type vibrotactile transducer. *The Journal of the Acoustical Society of America*, 128(2):619–627, 2010.

[73] T. Yan, A. Parri, V. Ruiz Garate, M. Cempini, R. Ronsse, and N. Vitiello. An oscillator-based smooth real-time estimate of gait phase for wearable robotics. *Autonomous Robots*, 41(3):759–774, 2017.

[74] R. Ronsse, S. M. M. De Rossi, N. Vitiello, T. Lenzi, M. C. Carrozza, and A. J. Ijspeert. Real-Time Estimate of Velocity and Acceleration of Quasi-Periodic Signals Using Adaptive Oscillators. *IEEE Transactions on Robotics*, 29(3):783–791, 2013.

[75] Y. Moon, R. McGinnis, K. Seagers, R. Motl, N. Sheth, J. Wright, R. Ghaffari, and J. Sosnoff. Monitoring gait in multiple sclerosis with novel wearable motion sensors. *PLOS ONE*, 12(2):e0171346, 2017.

[76] D. Thompson. Knee movement during the gait cycle. https://ouhsc.edu/bserdac/dthompso/web/gait/knmatics/kngait.htm, 1999.

[77] Y.-H. Kwon. Butterworth Digital Filters: Filter Function & Coefficients. http://www.kwon3d.com/theory/filtering/fil.html#coe, 1998.

[78] Laerd Statistics. Repeated Measures ANOVA. https://statistics.laerd.com/statistical-guides/repeated-measures-anova-statistical-guide.php.

[79] E. Buchanan. R - One-Way Repeated Measures ANOVA Example. https://www.youtube.com/watch?v=OeQqSZ6GJck, 2018.

[80] R. Mackenzie. One-Way vs Two-Way ANOVA: Differences, Assumptions and Hypotheses. https://www.technologynetworks.com/informatics/articles/one-way-vs-two-way-anova-definition-differences-assumptions-and-hypotheses-306, 2018.

[81] E. Buchanan. R - Two-Way Repeated Measures ANOVA Example. https://www.youtube.com/watch?v=Y1J5SWOy_Ro, 2018.

[82] Statistics Solutions. Paired Sample T-Test. https://www.statisticssolutions.com/manova-analysis-paired-sample-t-test/.

[83] S. Olney and J. Eng. Chapter 14: Gait. In *Joint Structure and Function: A Comprehensive Analysis*. 2010.

[84] S. Khandelwa and N. Wickström. Gait Event Detection in Real-World Environment for Long-Term Applications: Incorporating Domain Knowledge Into Time-Frequency Analysis. *IEEE Transactions on Neural Systems and Rehabilitation Engineering*, 2016.

[85] P. Lopez-Meyer, G. Fulk, and E. Sazonov. Automatic Detection of Temporal Gait Parameters in Poststroke Individuals. *IEEE transactions on information technology in biomedicine*, 15(4):594–601, 2011.

[86] Matlab. Zero-phase digital filtering. https://www.mathworks.com/help/signal/ref/filtfilt.html.

[87] M. Grimmer and A. Seyfarth. Mimicking Human-Like Leg Function in Prosthetic Limbs. In *Neuro-Robotics*, pages 105–155. Springer, Dordrecht, 2014.

[88] Laerd Statistics. Sphericity. https://statistics.laerd.com/statistical-guides/sphericity-statistical-guide.php.

[89] R. Rakotomalala. Test de normalité - Techniques empiriques et tests statistiques. Technical report, Université Lumière Lyon 2, 2011.

[90] Ressources Nationales de Chimie. Table de Shapiro et Wilk. http://eduscol.education.fr/rnchimie/math/benichou/tables/tshapiro/tshapiro.htm.

UNIVERSITÉ CATHOLIQUE DE LOUVAIN
École polytechnique de Louvain
Rue Archimède, 1 bte L6.11.01, 1348 Louvain-la-Neuve, Belgique | **www.uclouvain.be/epl**